CONTRACTORS REPORT
SERIES 90-16

Defence Research Establishment Pacific

Centre de recherches pour la défense pacifique

Arctic Ambient Noise and Modelling

Michael V. Greening

JASCO RESEARCH LTD.

Victoria, B.C.

for

DEFENCE RESEARCH ESTABLISHMENT PACIFIC

Research and Development Branch

Department of National Defence

Canada

Source Distribution

Michael V. Greening Jasco Research Ltd. 9865 West Saanich Rd., Sidney, British Columbia, Canada, V8L 3S1

Abstract

This report is an adendum to the two papers "Vertical Directivity Measurements of Ice Cracking" and "Extraction of the Seabed Reflectivity Function Using Ice Cracking as a Signal Source". This report presents the results completed, along with a description of the tasks remaining to obtain measurements of the spatial, strength and temporal distributions of the source. Upon completion of these results, the source model describing the total energy entering the water from ice cracking will be completed. This will then be combined with a propagation model to produce a noise model capable of reproducing various ambient noise features such as the coherence across a vertical array.

Introduction

The aim of this work is to produce a source model of low frequency ($\leq$ 200Hz) Arctic acoustic noise. This will then be combined with a propagation model to give a complete noise model capable of reproducing noise characteristics for any given Arctic environmental and propagation conditions.

The goal of the source model is to account for all energy entering the water from the ice. This requires knowledge of the source spectral shape, the source directivity, and the source distributions in space, strength and time. Both the energy entering the water in the vicinity of the source and that which may have propagated large distances through the ice and eventually leaked into the water should be included.

Due to the low sampling rate of 516Hz, the full spectral shape of ice cracking noise, which peaks near 200Hz - 300Hz, was not covered. However, the spectral shape measured at this low sampling rate has been shown in a previous report[1] and the full spectrum has been reported by other authors[2–4].

A complete analysis of the source directivity is available in the accompaning pa-

per "Vertical Directivity Measurements of Ice Cracking". This paper also addresses the relative importance of leaked plate waves in the ice and gives full details of the experimental setup, event detection and location techniques.

Thus, only the source distributions in space, strength and time are required to complete the source model. Results obtained to date on these distributions are given in this report.

Finally, although not required to model the source, it was found that the individual ice cracking events could be used to determine certain bottom characteristics such as the critical angle and the bottom loss above critical angle. This is shown in detail in the accompaning paper "Extraction of the Seabed Reflectivity Function Using Ice Cracking Noise as a Signal Source".

Results

A total of 916 individual ice cracking events were identified from 60 data files spanning a time of approximately 2.5 hours recorded over 6 days. The range, bearing, strength and times of all these events have been determined and are outlined in this report.

In determining the distribution in space of the events, both the range and bearing are required. The range of a source was determined using a ray tracing technique to calculate the propagation paths (direct arrival, bottom or surface reflection and multiple reflections) to all hydrophones on the vertical array. This is outlined in "Vertical Directivity Measurements of Ice Cracking". Ranges were determined to the nearest 10m for ranges out to 2km and to the nearest 50m for ranges out to 20km. However, large uncertainties in range may exist for events beyond 10km due to the large overlap in time of the various arrival paths. The bearing of a source was determined using only the direct arrival on the horizontal array and assuming straight ray theory. The ray tracing model was not used to determine bearing because the change in arrival times across the horizontal array are a function of both bearing and range. Tests at several angles showed a maximum error of approximately 10° between the straight ray and refracted ray theory for a source at 100m range. This was reduced to less than 1° for a source at 500m range. Thus, except for very close sources, the straight ray theory provides a very accurate fit to the array response of a transient. The bearing of each event was determined to the nearest increment of 5°.

Figures 1 and 2 show the measured spatial distributions of the source. These plots show that there are no prefered source locations or 'hot spots'. This supports the idea of a spatially isotropic noise field. However, assuming isotropy, the number of sources should increase with the square of the distance which does not occur in figures 1 or 2 and is not shown by the measured range distribution in figure 3. This is because these figures do not show all the events which occur but rather only those which are detected above the background noise. The number of sources detected will depend not only on the true range distribution, but also on the source directivity, source strength distribution, propagation loss, and the detection threshold. Thus, to verify the assumption of isotropy, the source directivity and strength distribution must be measured independently and included in a propagation model which will reproduce the measured source range distribution.

The source bearing distribution is also required to completely determine if the spatial distribution is isotropic. For a spatially isotropic noise field, the number of events is constant with changing direction. Thus, the measured bearing distribution, as shown if figure 4, does not appear consistant with an isotropic noise field. However, the major feature of this bearing distribution is the large decrease in the number of observed transients along the axis of the horizontal array (90° and 270°). This can be explained by the misinterpretation of low power events at endfire. Consider first a distant event occuring broadside to the horizontal array. For such an event, the length of the direct arrival from source to receiver is approximately equal for all hydrophones in the array. Thus, the direct arrivals line up in time and also contain the same energy when measured at each hydrophone across the array. This results in easy identification of the direct path and accurate measurement of the bearing. However, for an event occuring along the axis of the array, the direct arrival is well separated in time and contains different energy at each hydrophone due to the varying propagation path lengths. Thus, for an event with a low signal to noise ratio, the direct arrival may be mistaken for background noise at several of the hydrophones across the array. This produces an error in the bearing calculation resulting in an underestimate of the number of events along the axis of the array. Due to the large percentage of low power events (approximately 60% of the detected events have a signal to noise ratio of less than 3 dB), this can be a major source of error in the bearing distribution.

Thus, although the lack of any prefered locations in figures 1 and 2 support the spatially isotropic noise field assumption, this should be verified by comparing the measured range distribution with that produced by the completed noise model. Due to the easy misinterpretation of the bearing of an event occuring along the axis of the

array, the measured bearing distribution cannot be used to prove isotropy. However, if spatial isotropy is shown from the range distribution, the bearing distribution may be assumed to be flat.

In measuring the source strength distribution, only those events within 2km of the array are used. For these events, the direct arrival can be separated from other propagation paths and thus the source strength can be determined by measuring the power in the direct arrival and correcting for spherical spreading, source directivity and hydrophone gain. This has been performed on 160 of the approximately 400 events within 2km of the array. Completion of the remaining source strength measurements simply requires isolation of the direct arrival of these events and running this data through existing software. Although the measured source strengths have been corrected for propagation loss and source directivity, the detection threshold prevents low power events from being detected as their range increases. Thus the source strength distribution may be unreliable at the low power end. A method of correcting for this will be to examine the source strength distributions as a function of range within the 2km limit used. If possible, the source strength distribution as a function of time or temperature should also be examined.

Finally, the times of all 916 events have been recorded and the number of detected events ranged from 0 to 62 per two-minute sample of data. A plot of the distribution of the rate of detected events has not been produced and this should be related to the temperature.

References

1. M.Greening, "Arctic ambient noise beamforming and modelling," DREP internal report prepared for P.Zakarauskas, 31:03:1989.

2. A.R.Milne and J.H.Ganton, "Ambient noise under Arctic sea ice," J.Acoust.-Soc.Am., **36**, 855-863 (1964).

3. A.R.Milne, "Thermal tension cracking in sea ice: A source of underice noise," J.Geophys.Res., **77** (12), 2177-2192 (1972).

4. D.M.Farmer and Y.Xie, "The sound generated by propagating cracks in sea ice," J.Acoust.Soc.Am., **85** (4), 1489-1500 (1989).

Figure 1 Spatial Distribution of Sources

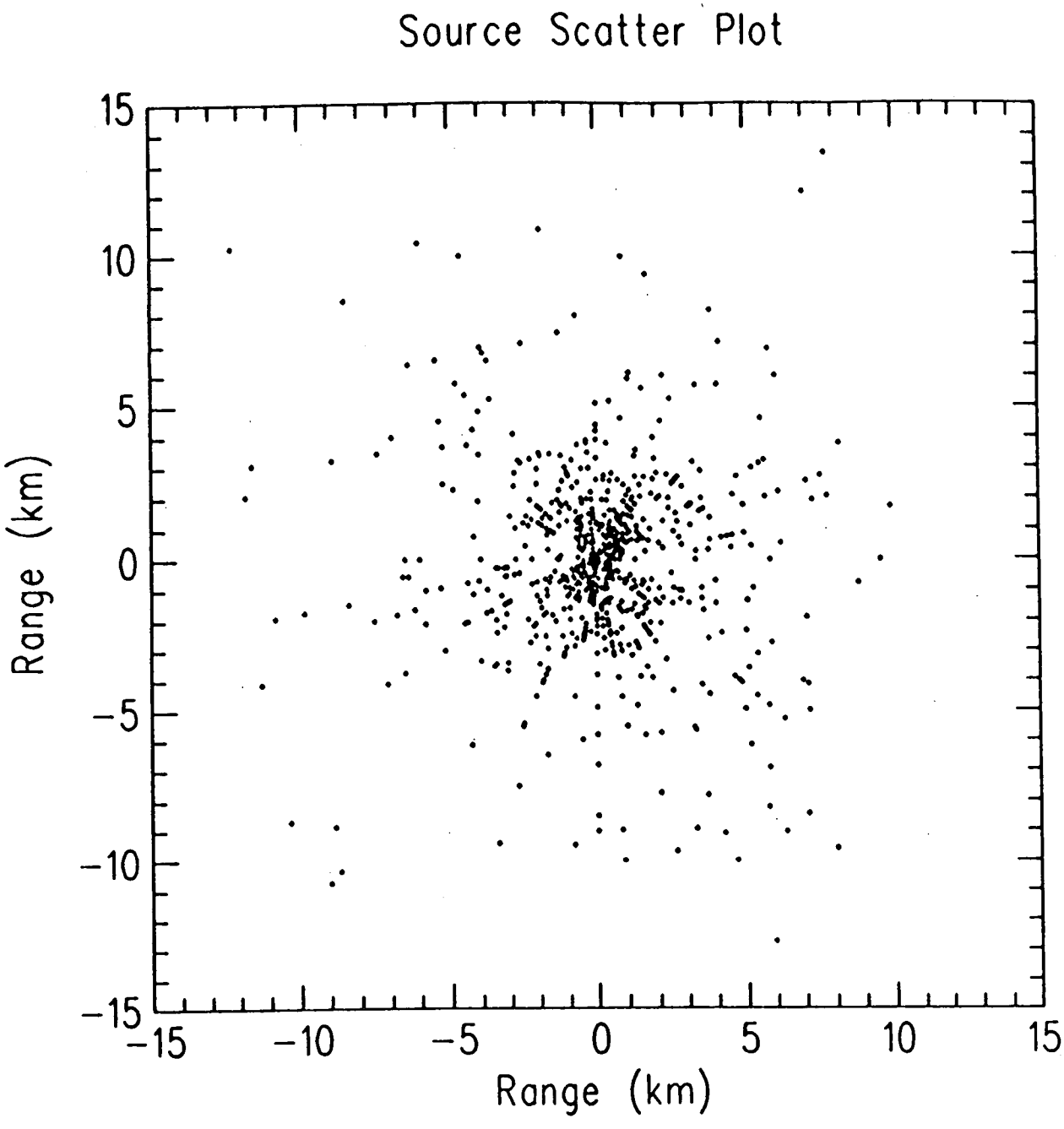

Figure 2 Spatial Distribution of Sources

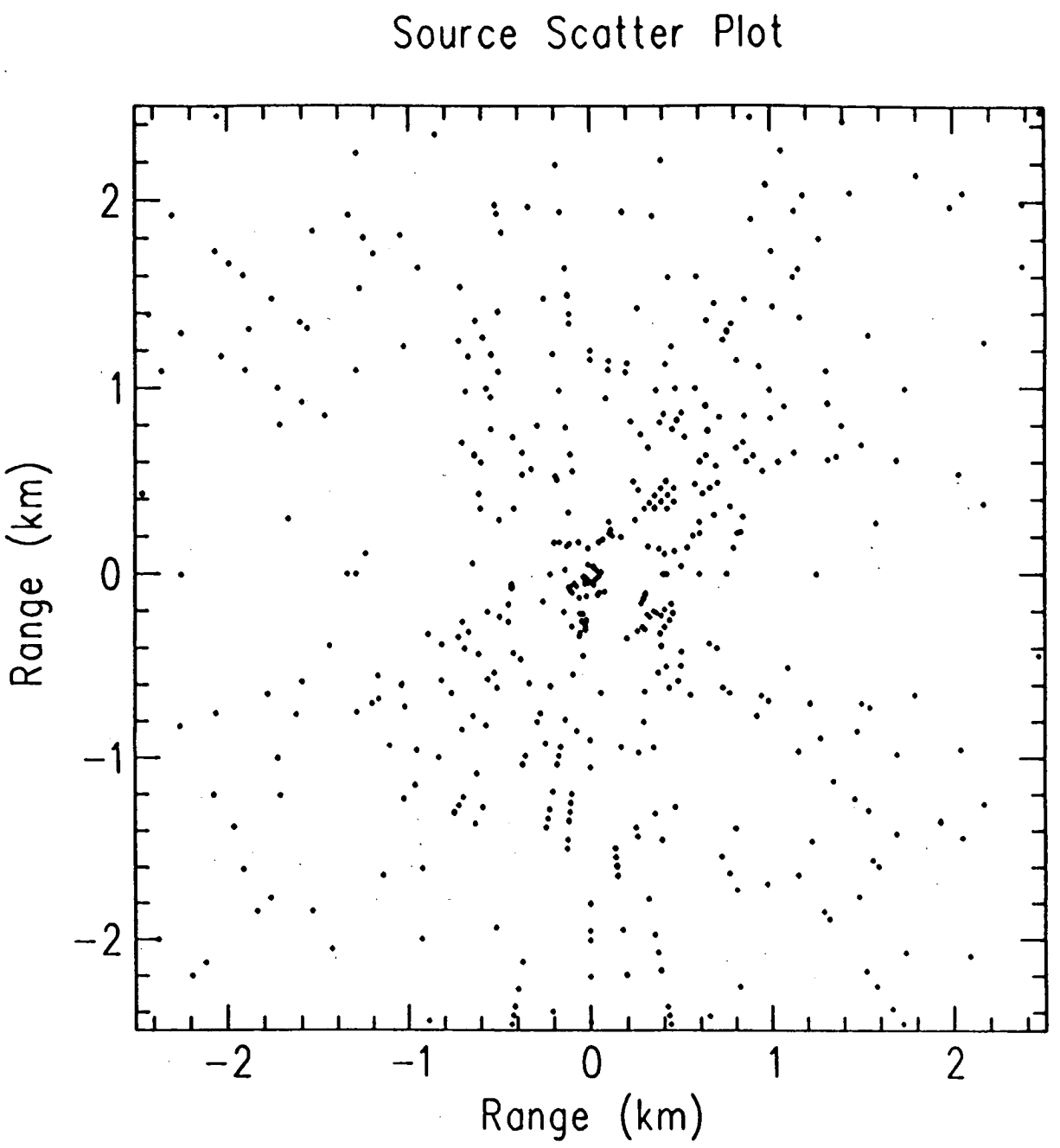

Figure 3

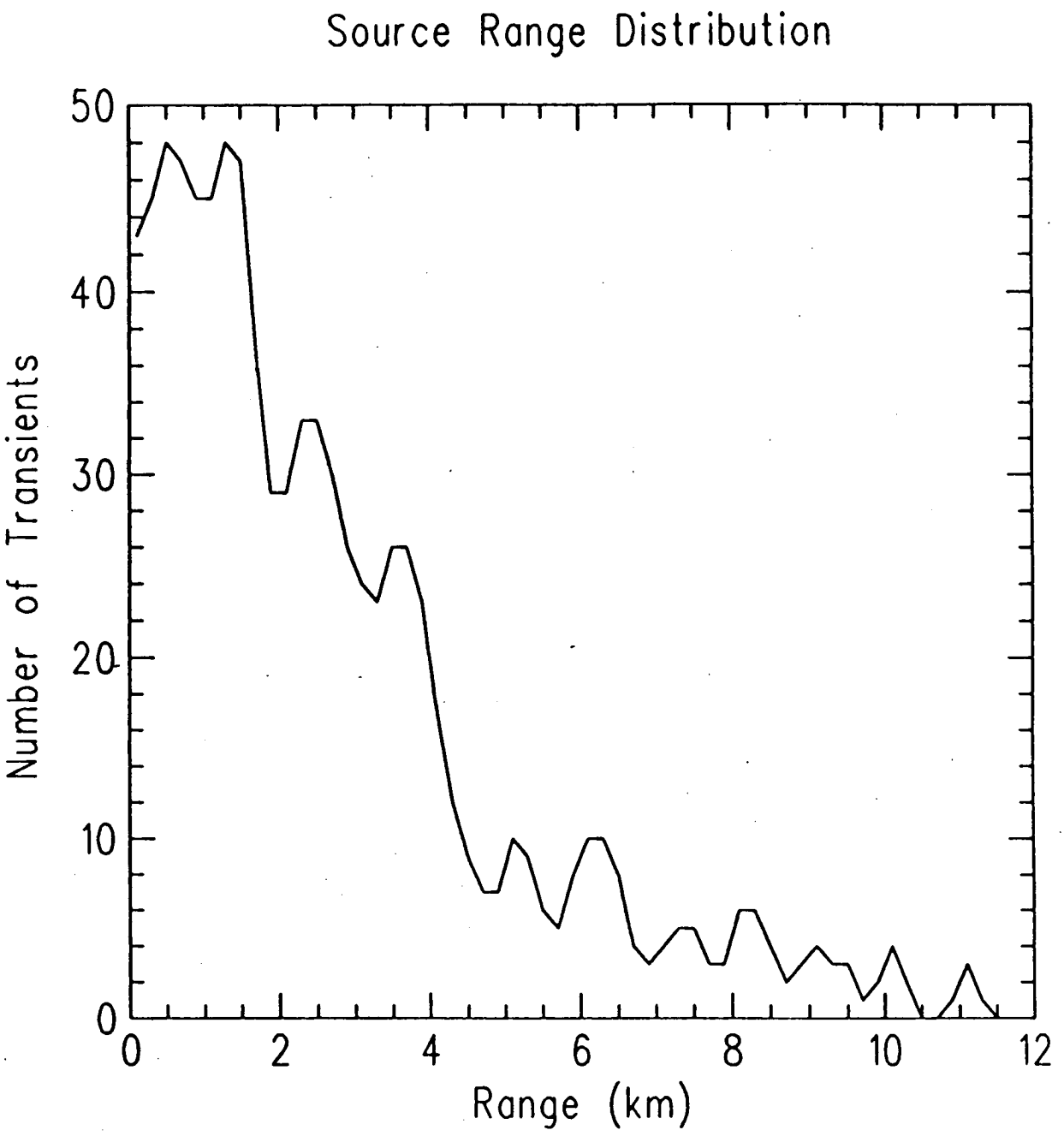
Source Range Distribution
Number of Transients
50
40
30
20
10
0
0
2
4
6
8
10
12
Range (km)

Figure 4

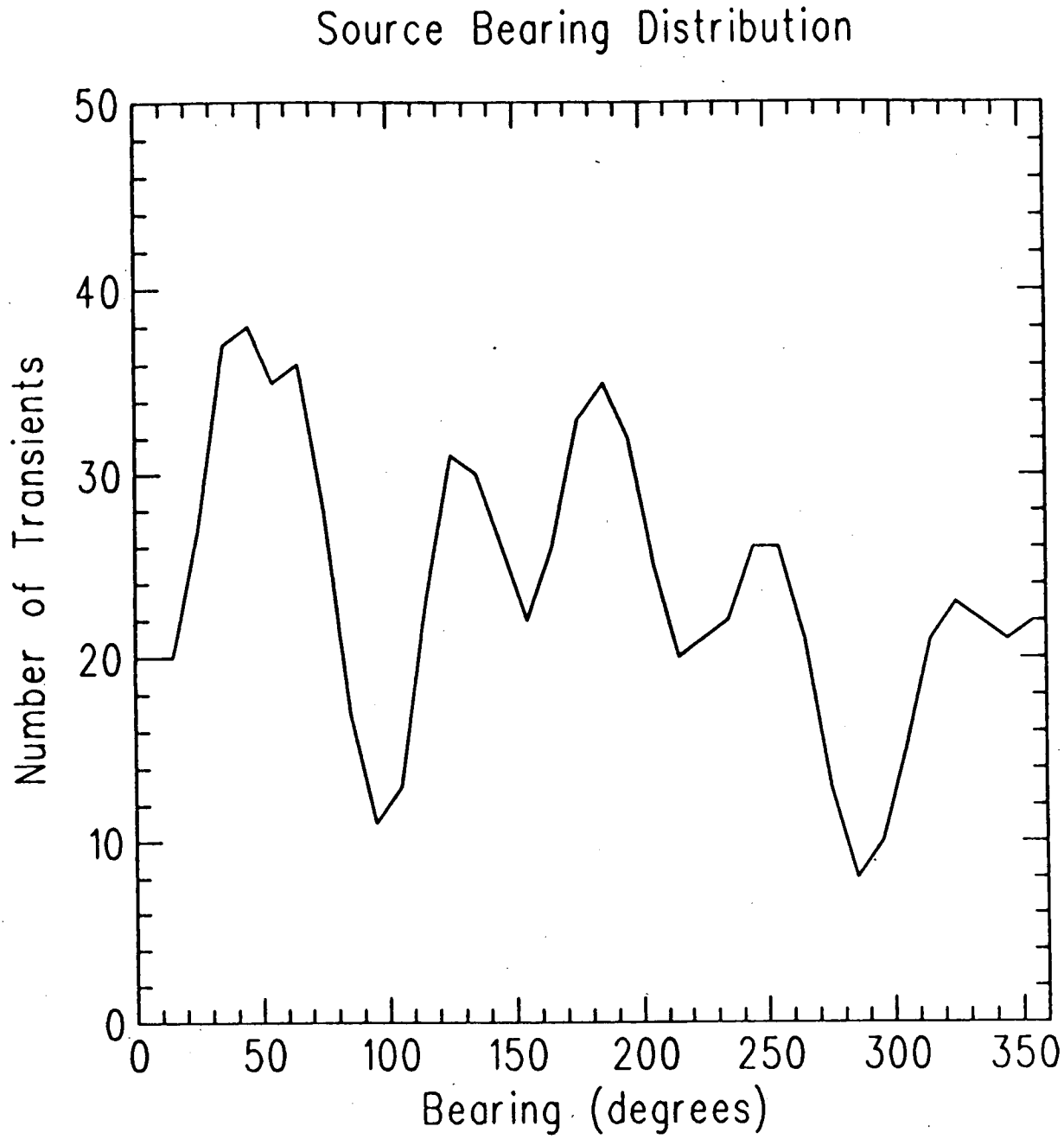
Source Bearing Distribution
Number of Transients
0
10
20
30
40
50
0
50
100
150
200
250
300
350
Bearing (degrees)

Vertical Directivity Measurements of Ice Cracking

Michael V. Greening Jasco Research Ltd. 9865 West Saanich Rd., Sidney, British Columbia, Canada, V8L 3S1

Pierre Zakarauskas, Ronald I. Verrall Defence Research Establishment Pacific, FMO, Victoria, British Columbia, Canada, V0S 1B0

This paper presents direct measurements of the vertical directivity of ice cracking events recorded on a 22 element vertical array deployed below the Arctic pack ice in 420 meters of water. The vertical directivity of ice cracking events is an important parameter in modelling Arctic ambient noise. Although it is often assumed to be a dipole or higher order multipole, very few field measurements exist. A total of 160 events spanning ranges of 40 m to 2000 m and source angles of 1° to 80° below horizontal are analyzed. The range of the source is determined by comparing the arrival times for the direct arrival and the multiple arrivals. The source strength is then determined using the power of the direct arrival only. Each hydrophone is associated with a different acoustic path and, therefore, a different source angle. The measured source pressure directivity, as determined from the 22 different angles, can be fitted accurately to a multipole of order m, although different events correspond to different values of m. The distribution of the order m for all the events has a positive skew with a mean of 0.80 and variance of 0.14. As the range of the source increases, both the skew and mean increase (with the mean always remaining below 1.0), while the variance decreases (eg. for events at 1300 m to 2000 m range, the mean was 0.88 with a variance of 0.10). Thus, the vertical directivity of thermal ice cracking events can be approximated as a dipole at far range.

I Introduction

It is generally assumed that the underwater ambient noise below 1000 Hz in the ice covered Arctic is dominated by ice cracking, either thermal or pressure ridging[1-4]. Thus a detailed model of these individual ice cracking events is required to understand the Arctic ambient noise. One very important characteristic of the source is its vertical directivity. The vertical directivity is simply a measure of the relative power radiated from a source as a function of elevation angle. Due to the high propagation loss associated with near vertical rays, long range propagation is restricted to angles near horizontal. Thus, the source directivity at these angles is critical in modelling the ambient noise.

For the open ocean, a major source of noise is entrapped bubbles from rain or breaking waves. A spherical bubble which expands and contracts in the water radiates equal energy in all directions resulting in monopole radiation. When the bubble depth is small compared to the wavelength of the energy radiated, interference of the bubble with its image source above the surface results in dipole radiation. However, for a source in the ice, the radiation pattern measured in the water depends on the shape of the source, the elastic properties of the ice and the complicated interactions with the rough ice surface and ice bottom. Thus, there is no apparently obvious radiation pattern for a source in the ice and several theoretical models have been proposed[5-7]. Stein[5] predicts a dipole radiation by using a point source in the ice. Langley[6] predicts a higher order multipole radiation pattern by using an extended source in the ice. Superimposed on the radiation pattern of the acoustic mode is the contribution due to leaked plate waves. Kim[7] produces a combined mathematical and numerical model to find the radiation pattern of typical sources used in geophysical studies such as strike-slip, dip-slip and tensile cracks.

Observation of the number of detectable ice cracking events with range[8,9], the ratio of energy in the direct arrival versus bottom reflection[10], and the ratio of energy in a lead pressure ridge versus a floe pressure ridge[11] have shown that ice cracking rediates predominantly in the vertical direction. These papers all assume a dipole directivity to determine other characteristics of the source or propagation parameters. However, theory has not proven that a dipole directivity is the appropriate form to use. Also, the only direct measurements of the vertical directivity known to the authors (other than those shown in this paper) are those performed by Stein[5,12]. Stein shows the directivity of two events as measured on a 24 element horizontal array with a 1 km aperature. The low signal to noise ratio along with the

limited span of vertical source angles available from a horizontal array resulted in an inconclusive directivity measurement which neither supported nor contradicted a dipole model.

This paper presents direct measurements of the vertical directivity of 160 ice cracking events. These events were recorded on a 24 element vertical array and spanned source angles from 1° to 80° below horizontal. Only those events within 2 km of the array and with a minimum signal to noise ratio of 3 dB are used. The range of the source is determined by comparing arrival times between the direct arrival and multiple arrivals across the array. Each hydrophone in the array corresponds to a different acoustic path and, therefore, a different vertical source angle. Thus, by measuring the power in the direct arrival only and correcting for propagation loss and background noise, the source strength as a function of vertical angle is obtained for each event.

The vertical directivity of most events was found to accurately fit a multipole model given as $sin^m\theta$ where θ is the source angle from horizontal and m is the order of the multipole ($m = 1$ corresponds to a dipole). Although m varied slightly with individual events, the distribution of m always peaked just below 1.0 and fell off rapidly at 1.0. Both the variance and peak of the distribution of m was found to depend on frequency, the signal to noise ratio and the range of the source. This paper clearly shows that vertical directivity of ice cracking events approximates a dipole at far range.

II Method

A. Environment and Instrumentation

The data analyzed in this paper were collected on the pack ice off the northern coast of Ellesmere Island. The ice cover was very rough, consisting of a mixture of both new and multiyear ice. The ice thickness varied from approximately 2 m on leads to 7 m on plates and to larger values on ridges. The data were obtained over several days in the early spring during which time the ice cover was relatively stable. Air temperatures during this time ranged from -14° to -40° with times of both warming and cooling. This provides times of both relative quiet and intense thermal ice

cracking[1,2,13,14]. Snow cover was as high as two feet which would normally stop thermal ice cracking over flat ice[1,2]. However, in the rough pack ice, many areas remain exposed and thin cracks have even been reported in the vertical faces of upthrust blocks of ice[15].

A set of approximately 60 two-minute samples of ambient noise, obtained over several days during April 1988, are examined. A vertical array of 24 hydrophones along with a 7 hydrophone horizontal array was deployed below the Arctic pack ice in water of 420 m depth. The vertical array was linear equispaced with a hydrophone separation of 12 m and the top hydrophone 18 m below sea level. The horizontal array was at 102 m depth and had a low redundancy spacing with an L shape, as shown in Fig. 1. A sampling rate of 516 Hz was used and the data was low pass filtered with a loss of 3 dB at 150 Hz and a further loss of 45 dB per octave.

B. Source Detection and Description

As stated in the introduction, the Arctic ambient noise is produced by the summation of individual transient noise sources produced by the ice. Detection of a transient source in a noisy background is a complex and common problem in most fields of signal processing and many techniques are available depending on the source and background characteristics. Two simple techniques were used to examine the data collected.

The first technique used was to scan the entire length (generally 2 minutes) of a single trace to determine the average voltage peak height, and then rescan the same trace while recording the position of all peaks greater than some user supplied multiple of the average peak height. Although this technique is not very robust, it was useful in finding the transient sources with a high signal to noise ratio.

Figs. 2 and 3 show the unprocessed output of the vertical array for two transient events at 480 m and 3150 m range respectively. (Note that channels 2 and 3 were not operating properly and thus were not used in any further processing of the data.) These figures clearly show multipath arrivals corresponding to a direct path, bottom reflection, bottom and underice reflection and multiple reflections from the bottom and ice. The range of a source was determined using a ray tracing model which calculates the eigenrays (the acoustic rays joining a source to a target) for a range independent, vertically stratified fluid with a flat bottom and surface. The

measured sound speed profile along with the approximate profile used for the ray model are shown in Fig. 4 while Fig. 5 shows an example of the eigenrays joining a surface source at a range of 5000 m to the 294 m deep hydrophone. Thus, the calculated arrival times of the eigenrays are compared with the array output for a given transient to determine the source range.

Close inspection of the transients in Figs. 2 and 3 show that an ice cracking event may contain several successive high amplitude peaks. These may correspond to a single arrival path such as for the 480 m range source in Fig. 2 or to a combination of several arrival paths which have been compressed in time as for the 3150 m range source in Fig. 3. This observation led to development of a second detection technique[16] which calculates the probability of finding x values out of a subsample of length y within the top fraction N of a sample z. This is a standard statistical method given by the formula:

$$P(x, y, N) = \sum_{i=x}^{y} \frac{y!}{i!(y-i)!} N^i \, (1-N)^{y-i}$$

Thus, by scanning the full length of data for one channel, a distribution of peak heights can be obtained which is then used on a second scan of the data to find all subsections of data of length y with x peaks within the top fraction N of the peak heights. By adjusting x, y and N to detect all transients in a section of data which has been visually examined, these values can then be used to detect transient events in all the data.

Over 900 ice cracking events were detected using the above procedure and visual confirmation of each event showed that the false alarm rate was less that 10%. Visual confirmation was performed using the entire vertical array and a false alarm is defined as an event for which no arrival paths can be seen across the array. This can be caused by fluctuations in the background noise level over the length of a two minute sample. Visual examination of the entire length of three data files containing 0, 18 and 62 transients showed that over 90% of the total observed ice cracking events were detected. Of all the events detected, only those with at least a 3 dB signal to noise ratio and for which the direct arrival could be separated in time from the bottom reflection or multiple reflections were used. The latter condition restricted the useful events to those within 2 km of the vertical array. This restriction combined with the required 3 dB signal to noise ratio reduced the number of useful events to 160. Of these, only 60 events had greater than a 15 dB

signal to noise ratio with a maximum of just over 30 dB. Powers were determined by summing over a one octave band centered at 96 Hz.

Power spectra of the direct arrival only for these ice cracking events peaked near 150 Hz which differs from the 200 Hz - 300 Hz peak as observed by previous authors[1,2,11]. This shift is due to the anti-aliasing low pass filters. The peak of the power spectra of the entire length of an event, including sea floor and underice reflections shifts towards lower frequency as the range of the source increases. This shift produced a maximum in the power spectra at a frequency as low as 50 Hz for events greater than 5 km range. This is due to the low pass filtering effect of reflection from the ice undersurface[17].

Several of the events detected using the first detection technique were markedly different from those shown in Figs. 2 and 3. These events have no discernable independent arrivals (such as direct path, bottom or underice reflections), extend over longer periods of time than the ice cracking events previously shown, and have characteristics of modal propagation such as nulls and phase changes with changing depth as shown in Fig. 6. Although the exact range of these events could not be determined because of the lack of individual arrivals, their modal properties indicate that these are very distant events. These events were found to have a maximum power near 20 Hz with a bandwidth of approximately 20 Hz. Thus, this may correspond to the low frequency Arctic pack ice noise reported by Dyer[4,18] and Makris and Dyer[19]. Because the range of the source is required to determine the directivity, these events were not used in any further processing and the data was high pass filtered at 30 Hz before the second detection method was used.

Finally, an arrival due to leakage of the longitudinal plate wave in the ice was also seen as a precursor to the acoustic mode for several events as shown in Fig. 7. The leaked plate wave arrival was present only on a small number of the close range transients (usually less than 1 km range). The absence of this arrival for far range and for other close range sources is due to absorption in the ice and scattering by discontinuities in the rough ice. The flexural plate wave which decays exponentially into the water was not seen on any of the data. Thus, the total energy in the water is produced mainly by the acoustic mode (energy entering the water in the vicinity of the source) while contributions due to leaked plate waves propagating in the ice are very small (but measurable). This agrees with previous observations[5,11,12].

C. Source Directivity

The vertical directivity of a source is a measure of the relative power radiated from the source as a function of angle from horizontal. Thus, by measuring the ratio of power in the direct arrival at several hydrophones (after correcting for propagation loss), the directivity can be determined. Fig. 8 shows the directivity patterns for a monopole, dipole and quadrupole source. For the rays joining the source to the two receivers shown, the ratio of the lengths from the source to a given directivity pattern (indicated by the changing thickness of the lines) shows the ratio of power received by the two hydrophones after correction for geometrical spreading. For the position of the receivers shown in Fig. 8, the ratio of these lengths is 1:1 for the monopole, 1:2 for the dipole and 1:4 for the quadrupole. Thus, if the source is a monopole, the two receivers will measure the same power (after correction for propagation loss). However, receiver 1 will be 3 dB lower than receiver 2 if the source is a dipole and 6 db lower if the source is a quadrupole. This gives the ratio of powers for any two receivers at the same angle from horizontal as for receivers 1 and 2 in Fig. 8. However, many directivity patterns could reproduce the same power ratio for these two angles and a measure of several angles from horizontal is required to determine the complete directivity pattern.

The vertical directivity of an individual ice cracking event was obtained in the following manner. An event is first identified and isolated as described previously. The received power in the direct arrival only is then measured for each hydrophone. This power measurement must then be corrected for both propagation loss and background noise. The noise is removed by subtracting the power contained in an equal length of data immediately preceeding the direct arrival. For our measurements, the noise power was only sampled at one hydrophone and assumed constant along the array. Finally, by using the direct arrival only, the propagation loss may be calculated by correcting for spherical spreading only, without reflections from the bottom or surface. Absorption can be ignored as it is insignificant (approximately 10^{-3} dB/km at 100 Hz) for these short ranges and low frequencies[20]. The spherical spreading loss is easily obtained by using the ray tracing model to calculate the propagation path lengths for the direct arrival to all hydrophones in the vertical array. This ray tracing technique also yields the vertical source angles to each hydrophone and thus, the power radiated by the source at these angles is obtained.

For a given ice cracking event, the measured vertical directivity was fitted to a multipole model given as $P_r = Psin^m\theta$ where P_r is the received power at source

angle θ, m is the order of the multipole ($m = 1$ corresponds to a dipole) and P is the power of the source. Thus, P and m may be determined using a linear least squares fit in the log of P_r versus $sin\theta$. Figs. 9a and 9b show the measured directivity of two ice cracking events as a function of source angle along with the directivity patterns calculated using the multipole model. These figures clearly show that the multipole model fits these events very well and that the order of the multipole is not necessarily unity. Sources of error may be caused by several factors. First, the small sampling rate of 516 Hz results in direct arrivals with lengths of only 70 to 120 data points depending on source range. Power spectra from such short data samples are subject to fluctuations and thus, all events were summed over a one octave band centered at 96 Hz to help reduce this error. A second source of error is caused by the convergence or divergence of rays in a refractive medium, which has not been included in the propagation loss. Finally, a small frequency dependent fluctuation in gain of the order of 0.5 - 1 dB was found in several hydrophones.

Of the 160 ice cracking events examined, 95 or approximately 60% were found to fit the multipole model with a random average deviation of less than 1.5 dB per hydrophone. These small deviations are assumed to be caused mainly by the short data length, refraction effects and gain error as described above. A further 42 events (approximately 26%) were found to fit the multipole model with an average deviation of between 1.5 dB - 3.0 dB. Examination of these events showed that the deviations from the multipole were no longer random but instead followed some pattern as shown by the two events in Figs. 10a and 10b. These small fluctuations from a multipole are assumed to be caused by either the shape of the source, some anisotropic feature of the ice, or the reflection and transmission properties at the air and water boundaries of the ice. Although the multipole model will not account for these fluctuations, it provides a very good first estimate of the directivity of these events and thus was still used to model these events. The remaining 23 events (approximately 14%) were found to have complex directivity patterns as shown by the two examples in Fig. 11. Although a multipole fit is shown, the fit is meaningless and these events were not used in any further processing. The complex directivity of these events is assumed to be caused by either the shape of the source or some large anisotropic feature of the ice at the location of the source such as the keel of a pressure ridge.

III Results

It was shown in the previous section that a multipole model of the form $sin^m\theta$ provided a very good fit to approximately 86% of the 160 transient events analysed. However, the order m of the multipole was found to vary between individual events. The distribution of m for all 137 ice cracking events which fit the multipole model is shown in Fig. 12. This distribution has a positive skew with a mean of 0.80 and variance of 0.14. The distribution of m was also examined as a function of source range and is shown in Fig. 13 while table 1 shows the values of the mean, variance and skewness. It was found that in all cases, the distribution of m falls off rapidly near 1.0 with very few events above 1.5 and none above 2.5. It was also found that as the source range increases, the mean increases (always remaining below 1.0) while the variance decreases. At a source range of approximately 0 - 40 wavelengths, the directivity index m is still broadly distributed about a center near 0.65 while for source ranges of approximately 85 wavelengths or greater, the distribution narrows nearer 1.0. Thus, the vertical directivity of ice cracking events may be approximated as a dipole at far range and shifts closer to a monopole at close range.

The distribution of m was also examined as both a function of minimum signal to noise ratio and frequency as shown in Fig. 14 and 15. Frequencies were always averaged over an octave band centered on the frequency shown. Values of the mean, variance and skew for these distributions are also given in table 1. It was found that the mean increased as the frequency increased and also as the required signal to noise ratio decreased; again with the mean always remaining below 1.0. However, as the frequency increases, the range in wavelengths increases. Also, as the minimum signal to noise ratio increases, the number of far range events detected decreases due to the large propagation loss. Thus, these results of the distribution of m as a function of frequency or signal to noise ratio could both simply be due to the dependence on range.

Finally, although a multipole model was an accurate fit to 86% of the events identified, an increase in sound intensity of approximately 2 dB - 4 dB above this level was found centered about a 60° - 65° source angle. This increase can be seen on the directivity of the event shown in Fig. 10b. Although small fluctuations of a few dB were found on 30% of the 137 events used, an increase of 2 dB - 4 dB at 60° - 65° was found on 9 out of 13 or 70% of the events which had source angles this high. Thus, the increase in sound level at this angle can not be assumed to be due

to a random fluctuation. However, it is easily explained as the leaked plate wave which coincides with the acoustic wave at this angle and thus cannot be separated in time from the acoustic wave as it could in Fig. 6. Thus, this increase should be included in the directivity of the source and a proposed model of the vertical directivity is:

$$P_r = P \left[sin^m\theta + C\ exp\left[-\frac{(\theta - \theta_L)^2}{2w^2} \right] \right]$$

where C is a constant giving the relative contributions of the acoustic mode and the leaked longitudinal plate wave, and θ_L and w are the critical angle and beamwidth of the leaked longitudinal plate wave respectively. For our data, $C \approx 1.0$, $\theta_L \approx 60°$, and $w \approx 5°$. Note that the leaked longitudinal plate wave has little effect on the long range propagation if the bottom critical angle is below 60° from horizontal. Also, although the leaked plate wave contributes to the acoustic mode, it was noted earlier that as the range increases, this wave is rarely observed due to scattering and absorption in the ice.

IV Discussion and Conclusions

This paper has shown through field measurements that the vertical directivity of ice cracking in the Arctic pack ice approximates a dipole radiation pattern for far range and shifts towards a monopole for close range. The observed dipole radiation agrees with Stein's theoretical model of a monopole source in the ice[5]. Superimposed on this radiation pattern is a small 2 dB - 4 dB increase in level near 60° - 65° due to the leaked longitudinal plate wave coinciding with the acoustic mode at these source angles. Contributions from the leaked longitudinal plate wave away from the source rapidly disappear due to scattering and absorption in the ice.

The directivity index m was also found to increase with both an increasing frequency and a decreasing detection threshold or minimum signal to noise ratio. However, both these dependencies may be a result of the range dependence.

V References

1. A.R.Milne and J.H.Ganton, "Ambient noise under Arctic sea ice," J.Acoust.-Soc.Am., **36**, 855-863 (1964).

2. A.R.Milne, "Thermal tension cracking in sea ice: A source of underice noise," J.Geophys.Res., **77** (12), 2177-2192 (1972).

3. R.S.Pritchard, "Arctic Ocean background noise caused by ridging of sea ice," J.Acoust.Soc.Am., **75** (2), 419-427 (1984).

4. I.Dyer, "Ice source mechanisms: speculation on the origin of low frequency Arctic ocean noise," in *Proceedings of the Natural Mechanisms of Surface Generated Noise in the Ocean,* NATO A.R.W., Lerici, Italy, June 1987.

5. P.J.Stein, "Acoustic monopole in a floating ice plate," Doctoral thesis, Department of Ocean Engineering, MIT., Cambridge, Woods Hole Oceanographic Institution, Woods Hole, Massachusetts, 1986.

6. A.J.Langley, "Acoustic emission from the Arctic ice sheet," J.Acoust.Soc.Am., **85** (2), 692-701 (1989).

7. J.S.Kim, "Radiation from directional seismic sources in laterally stratified media with application to Arctic ice cracking noise," Doctoral thesis, Department of Ocean Engineering, MIT., Cambridge, Massachusetts, 1989.

8. A.R.Milne, "Statistical description of noise under shore-fast sea ice in winter," J.Acoust.Soc.Am., **39** (6), 1174-1182 (1966).

9. M.Townsend-Manning, "Analysis of central Arctic noise events," Master's Thesis, Department of Ocean Engineering, MIT., Cambridge, Massachusetts, 1987.

10. D.M.Farmer and Y.Xie, "The sound generated by propagating cracks in sea ice," J.Acoust.Soc.Am., **85** (4), 1489-1500 (1989).

11. B.M.Buck and J.H.Wilson, "Nearfield noise measurements from an Arctic pressure ridge," J.Acoust.Soc.Am., **80** (1), 256-264 (1986).

12. P.J.Stein, "Interpretation of a few ice event transients," J.Acoust.Soc.Am., **83** (2), 617-622 (1988).

13. J.H.Ganton and A.R.Milne, "Temperature-and wind-dependent ambient noise under midwinter pack ice," J.Acoust.Soc.Am., **38** (3), 406-411 (1965).

14. A.R.Milne, J.H.Ganton and D.J.McMillin, "Ambient noise under sea ice and further measurements of wind and temperature dependence," J.Acoust.Soc.-Am., **41** (2), 525-528 (1967).

15. P.Zakarauskas and J.M.Thorleifson, "Directionality of ice cracking events," Submitted to J.Acoust.Soc.Am., 1990.

16. P.Zakarauskas, C.J.Parfitt and J.M.Thorleifson, "Statistics of transients in Arctic ambient noise," To be published in *Proceedings of the First French Conference on Acoustics,* Lyon, France, 1990.

17. T.C.Yang and C.W.Votaw, "Under ice reflectivities at frequencies below - 1kHz," J.Acoust.Soc.Am., **70** (3), 841-851 (1981).

18. I.Dyer, "The song of sea ice and other Arctic Ocean melodies," in *Arctic Technology and Policy,* Hemisphere, Washington, D.C., 1983.

19. N.C.Makris and I.Dyer, "Environmental correlates of pack ice noise," J.Acoust.-Soc.Am., **79** (5), 1434-1440 (1986).

20. L.M.Brekhovskikh and Y.Lysanov, *Fundamentals of Ocean Acoustics,* Springer series in electrophysics, New York, 1982.

Range (m)	SNR (dB)	Frequency (Hz)	Mean	Variance	Skew
0-2000	3	96.7	0.80	0.14	0.78
0-650	3	96.7	0.65	0.14	1.35
650-1300	3	96.7	0.83	0.12	0.32
1300-2000	3	96.7	0.88	0.10	0.88
0-2000	3	96.7	0.80	0.14	0.78
0-2000	7	96.7	0.71	0.14	0.85
0-2000	10	96.7	0.66	0.14	0.75
0-2000	3	48.4	0.70	0.15	0.79
0-2000	3	96.7	0.80	0.14	0.78
0-2000	3	145.1	0.92	0.18	0.29

Table 1 Mean, Variance and Skew for Distributions of m as a Function of Range, Signal to Noise Ratio and Frequency

Extraction of the seabed reflectivity function using ice cracking noise as a signal source

Pierre Zakarauskas, Ronald I. Verrall
(Defence Research Establishment Pacific, FMO, Victoria, British Columbia, Canada, VOS 1B0)

Michael V. Greening
(Jasco Research Ltd. 9865 West Saanich Rd., Sidney, British Columbia, Canada, V8L 3S1)

ABSTRACT

A technique is described for measuring the reflection coefficient of the Arctic seabed with a single vertical array of hydrophones. Naturally occurring ice cracks were used as the acoustic sources. This method circumvents the difficulties and expense of introducing artificial sound sources through the thick Arctic pack ice. The measurements were made in April 1988, with a 22-element array suspended from the ice in 420 meters of water. The range of the source is first determined using the direct arrival and multiple reflections from the seabed and underice surface. Then the directivity index is determined using the direct arrival path only. A plot of the reflection coefficient versus grazing angle clearly indicates the value of the critical angle. The sound speed of the sea bottom corresponding to this critical angle agrees well with that measured from a bottom grab sample taken during the field trip. Finally, an interesting phenomenon was an anomalous increase of power at a grazing angle of 60°. This is associated with a leaky plate wave radiating at the ice-water interface.

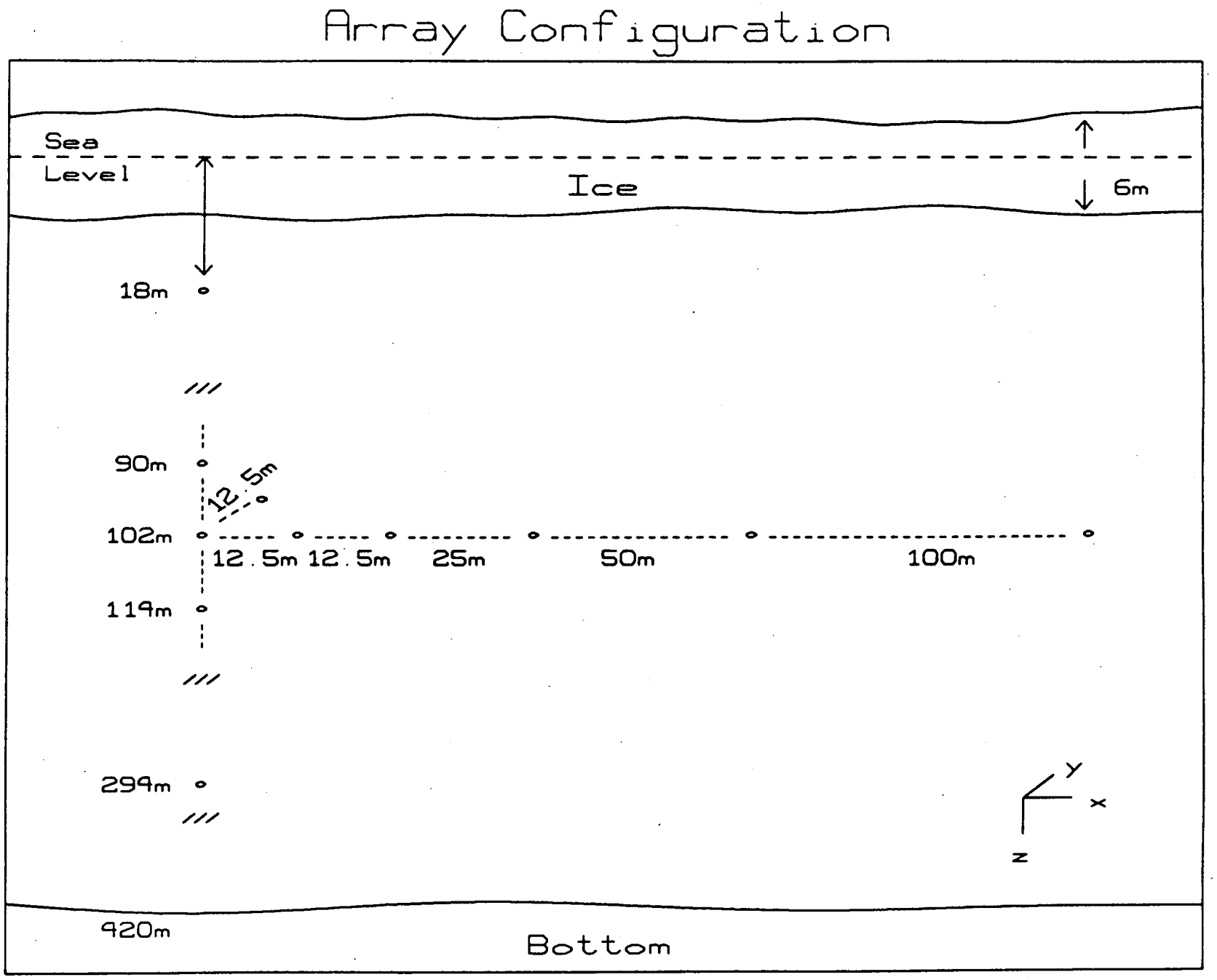
Array Configuration
Sea
Level
Ice
6m
18m
90m
12.5m
102m
12.5m
12.5m
25m
50m
100m
119m
294m
Y
X
Z
420m
Bottom

Figure 1

Figure 2 Ice Cracking Event
Source Range = 480m

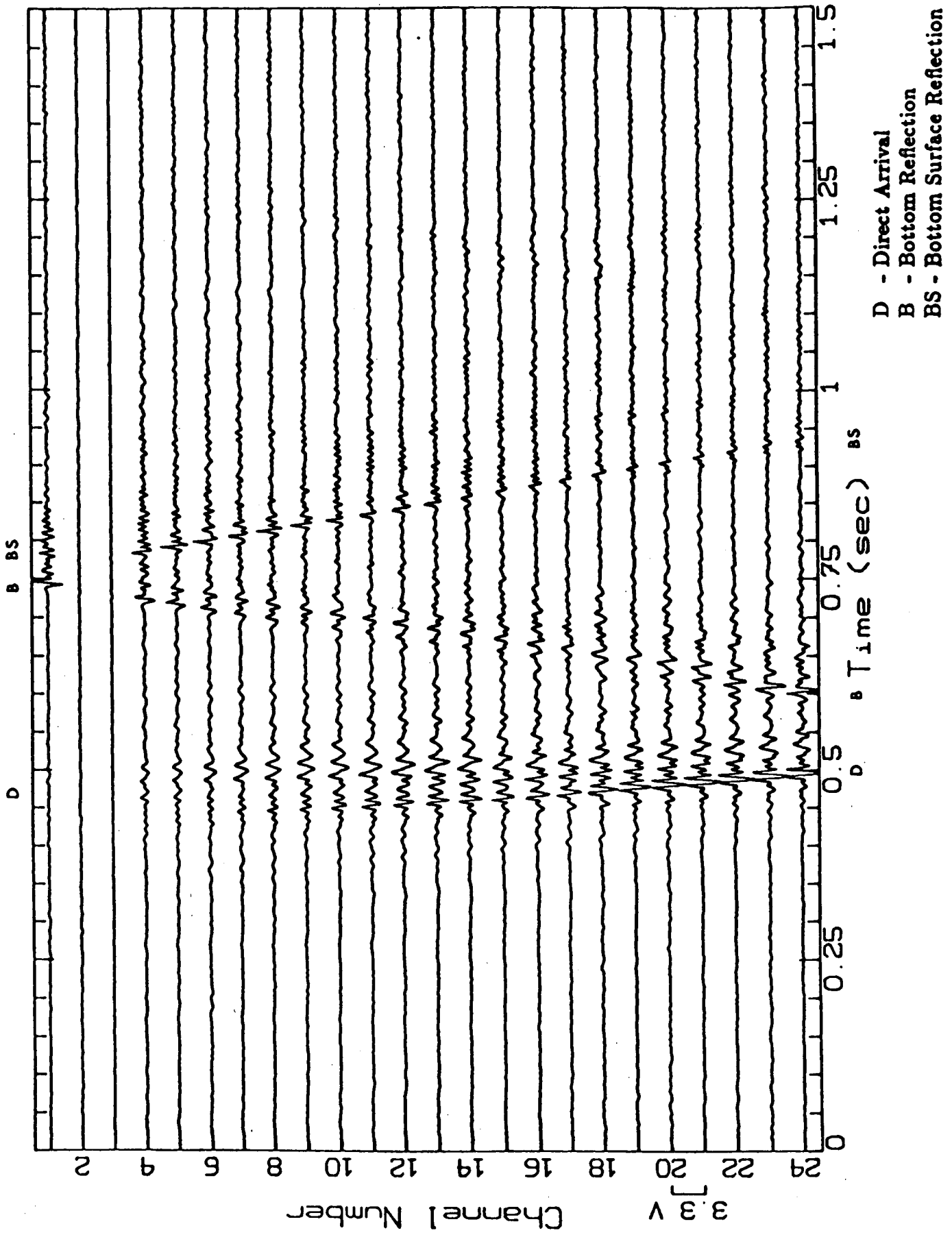

Figure 3 Ice Cracking Event
Source Range = 3150m

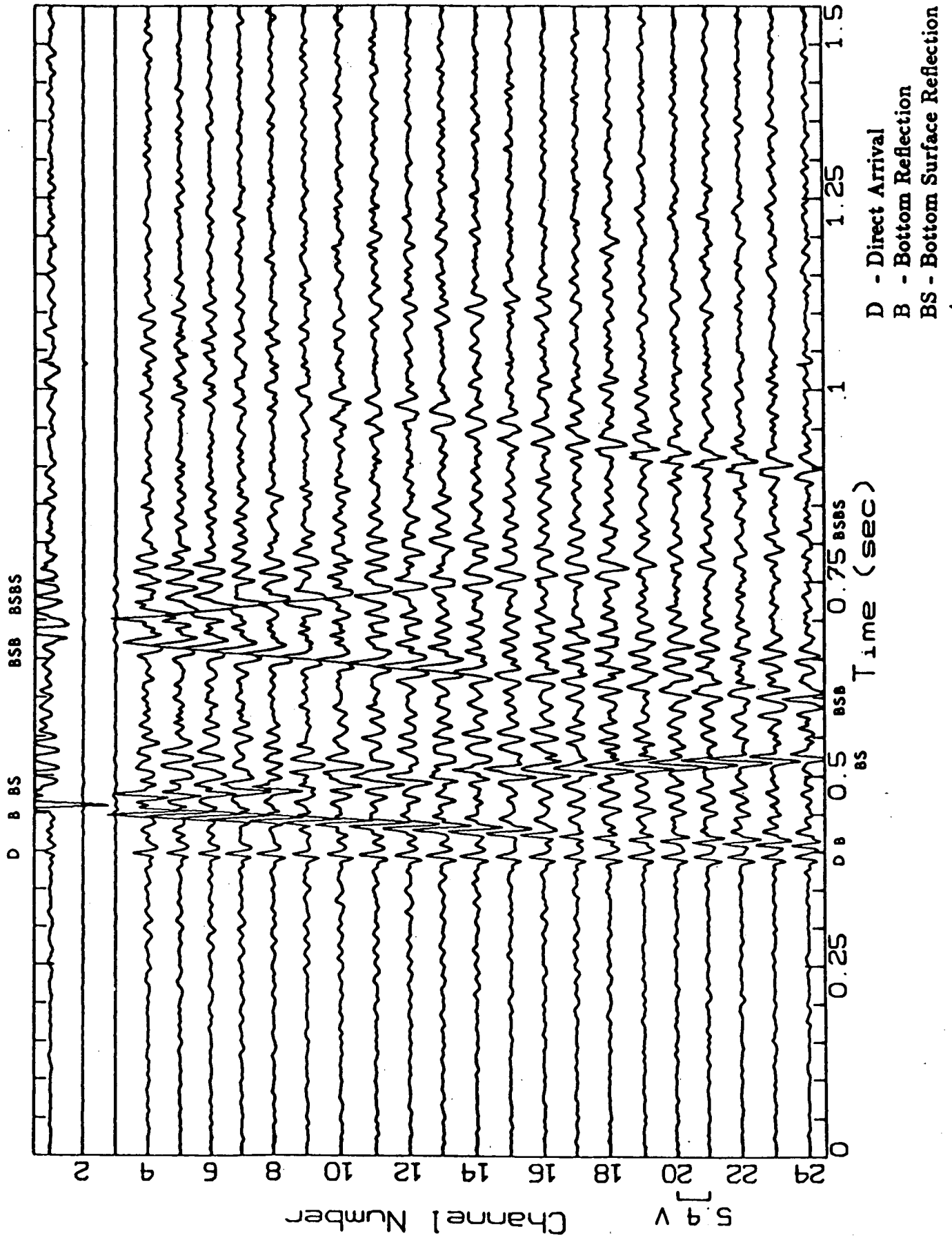

Figure 4

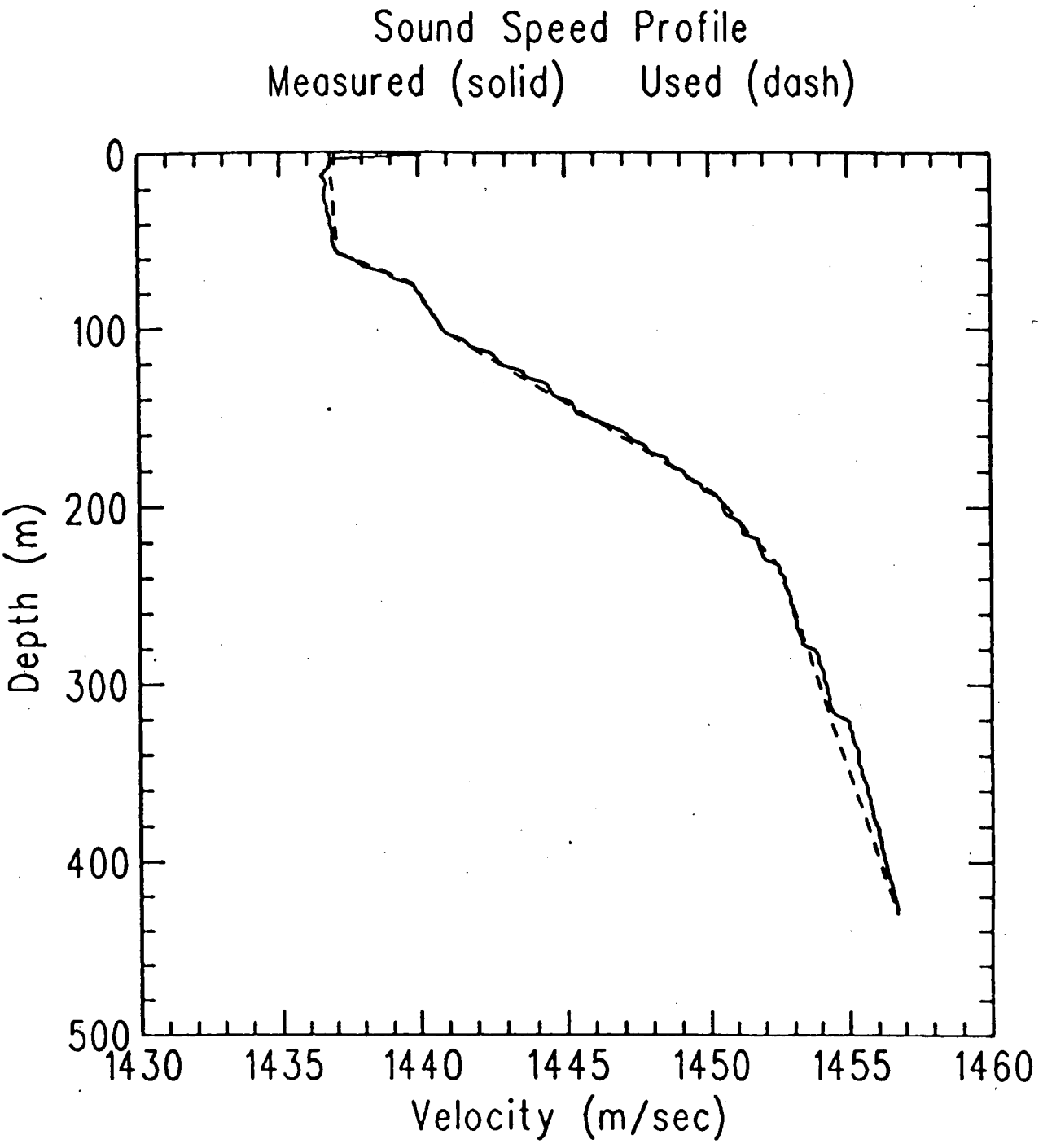
Sound Speed Profile
Measured (solid) Used (dash)
Depth (m)
0
100
200
300
400
500
1430
1435
1440
1445
1450
1455
1460
Velocity (m/sec)

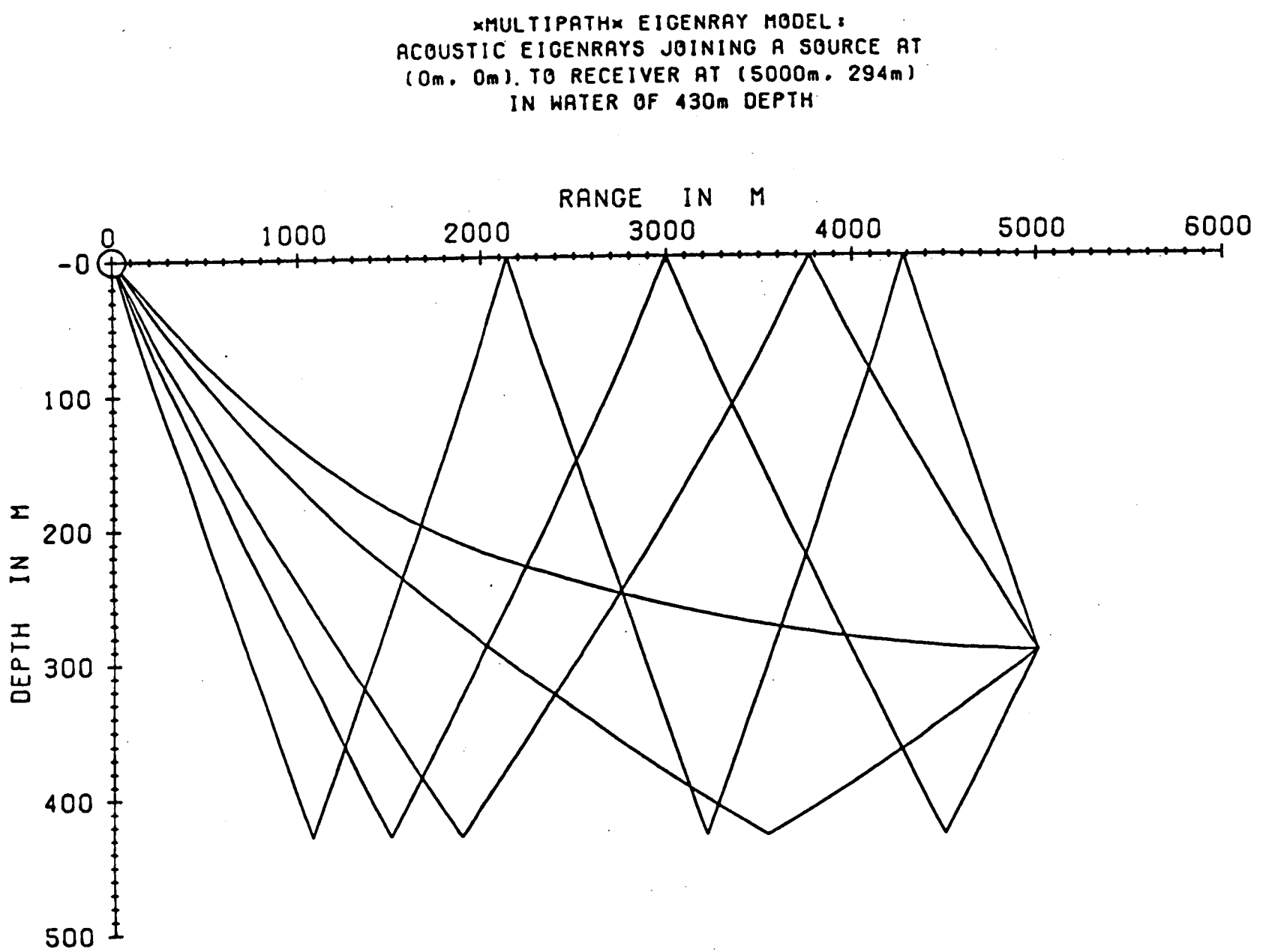
×MULTIPATH× EIGENRAY MODEL:
ACOUSTIC EIGENRAYS JOINING A SOURCE AT
(0m, 0m). TO RECEIVER AT (5000m, 294m)
IN WATER OF 430m DEPTH
RANGE IN M
0
1000
2000
3000
4000
5000
6000
-0
100
200
300
400
500
DEPTH IN M

Figure 5

Figure 6 Long Range Event
with Modal Properties

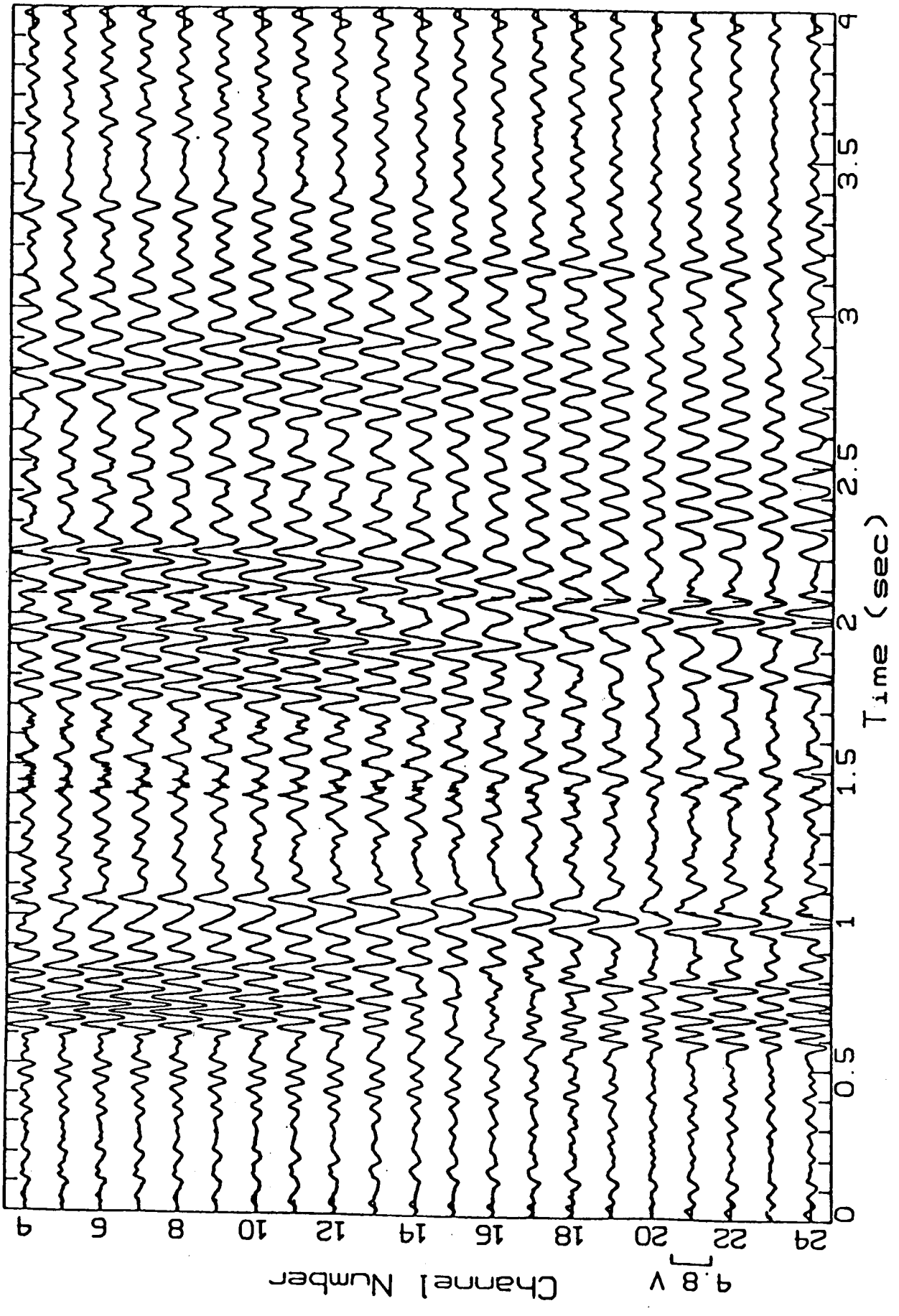

Figure 7 Ice Cracking Event with
Leaked Longitudinal Plate Wave
Source Range = 400 m

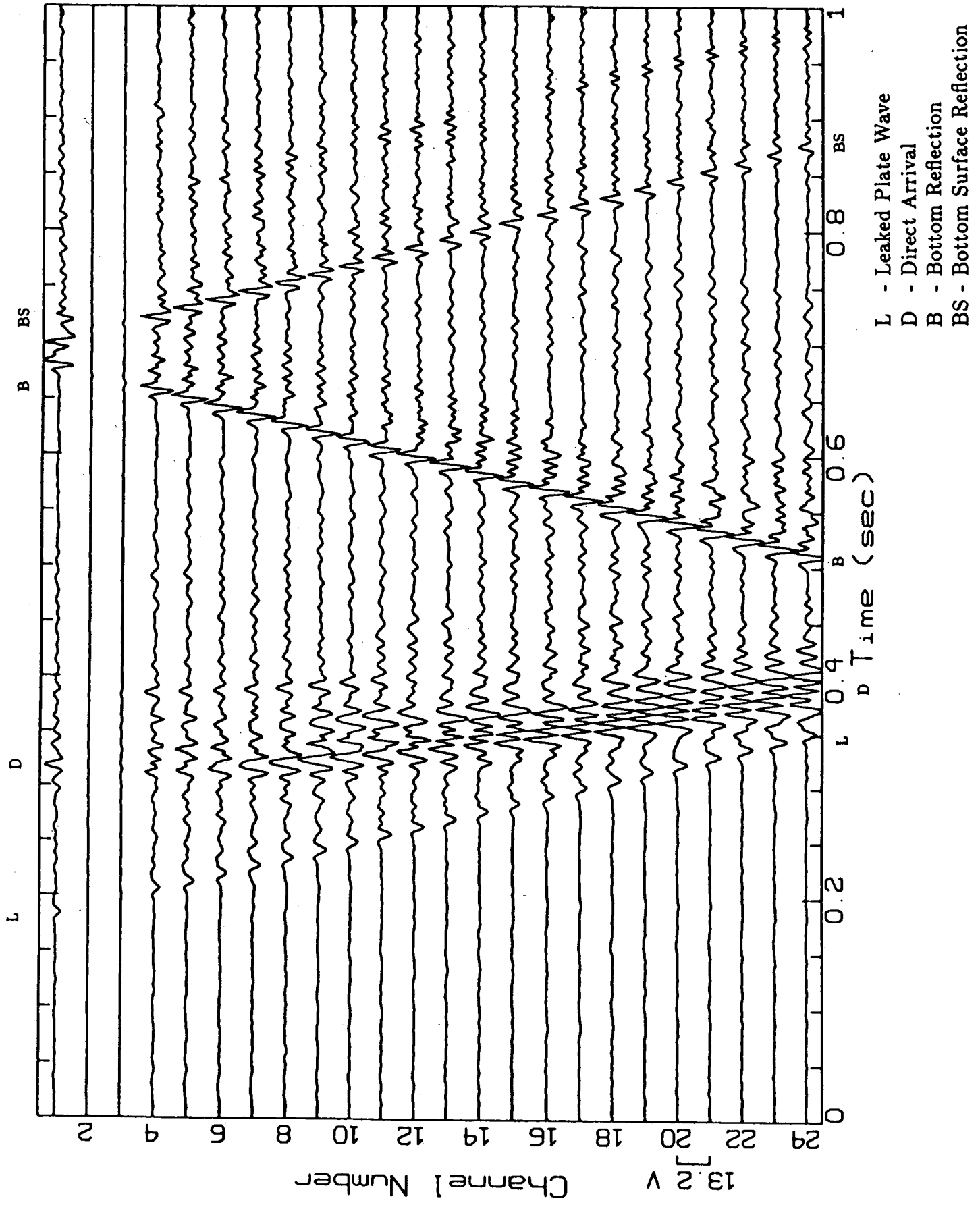

Figure 8 Directivity Patterns for
Monopole, Dipole and Quadupole
(Indicated by increasing thickness)

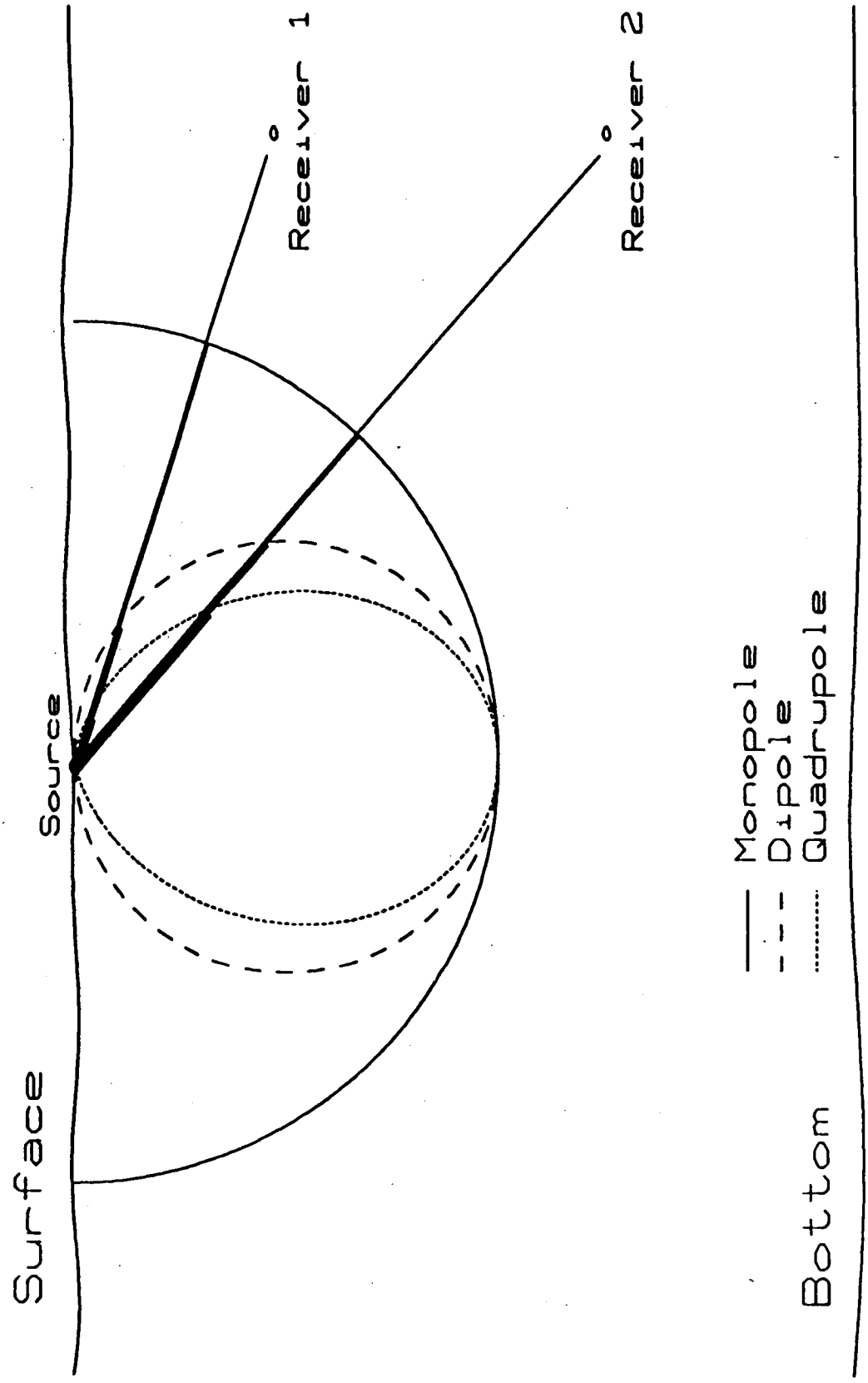

Figure 9a Directivity for Event at 1050m Range
Directivity Index $m = 0.94$

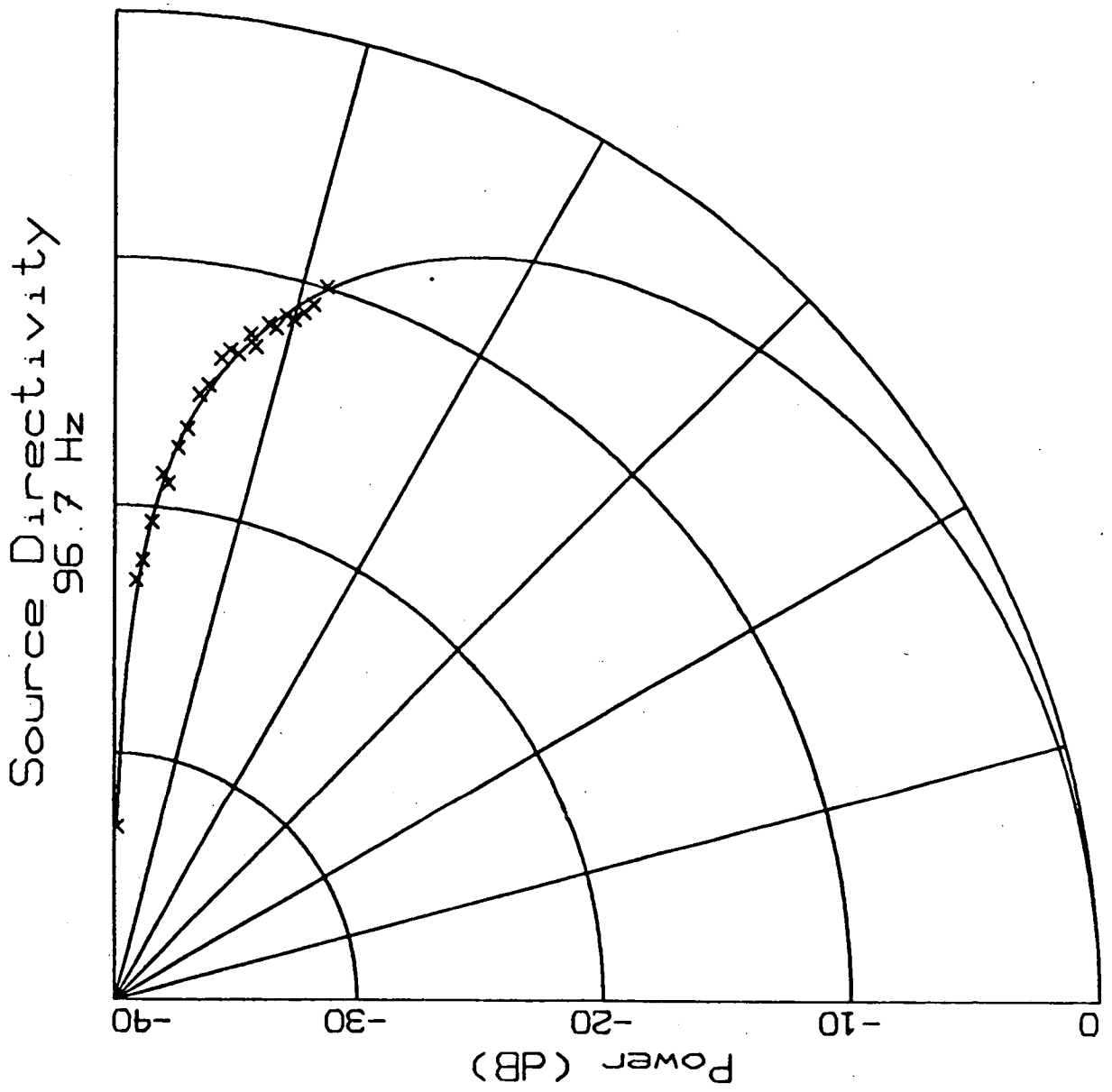

Figure 9b Directivity for Event at 450m Range
Directivity Index $m = 0.76$

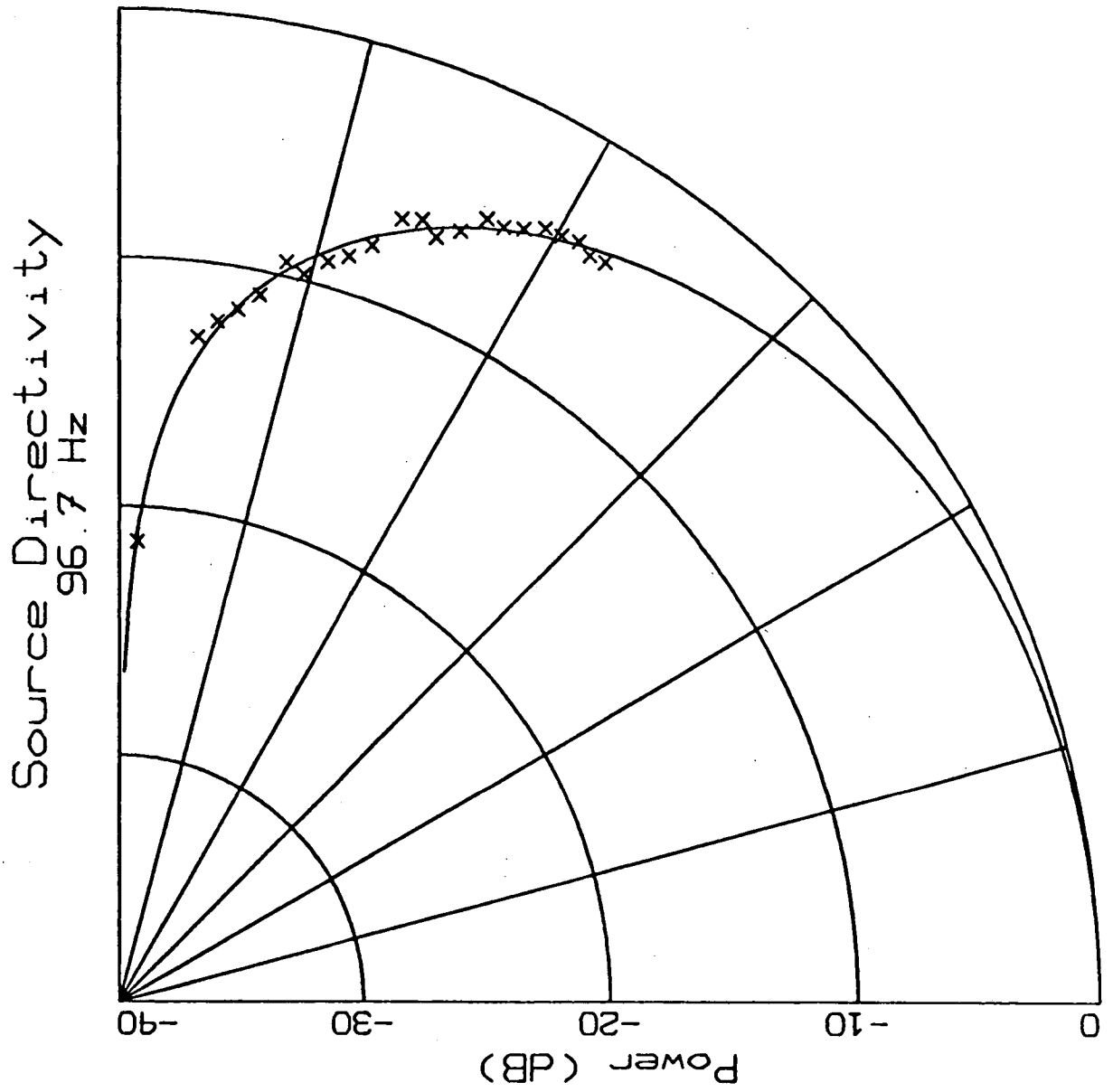

Figure 10a Directivity for Event at 300m Range
Showing Small Fluctuations from Pure Multipole
Directivity Index $m = 1.00$

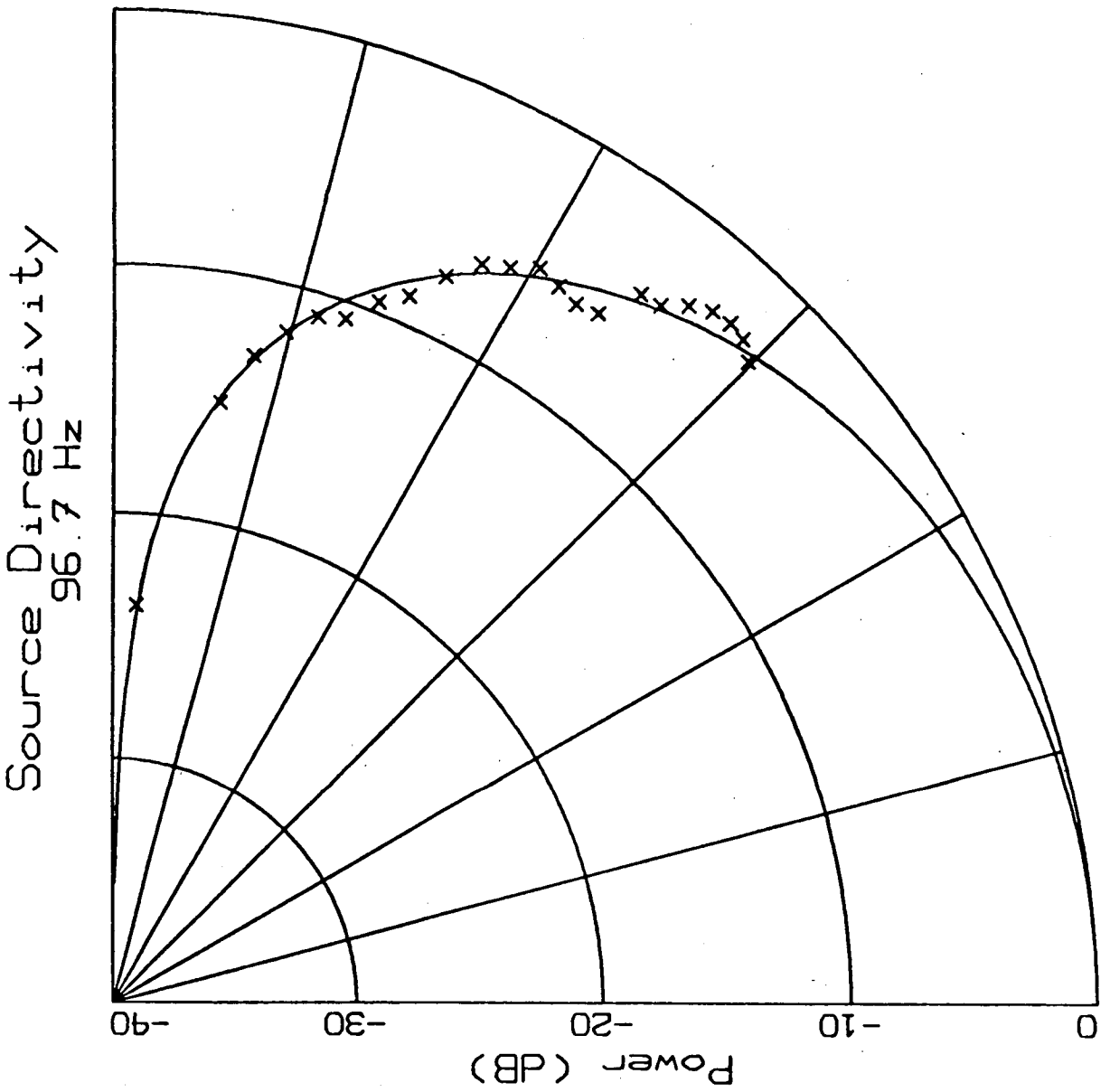

Figure 10b Directivity for Event at 120m Range
Showing Small Fluctuations from Pure Multipole
Directivity Index $m = 0.51$

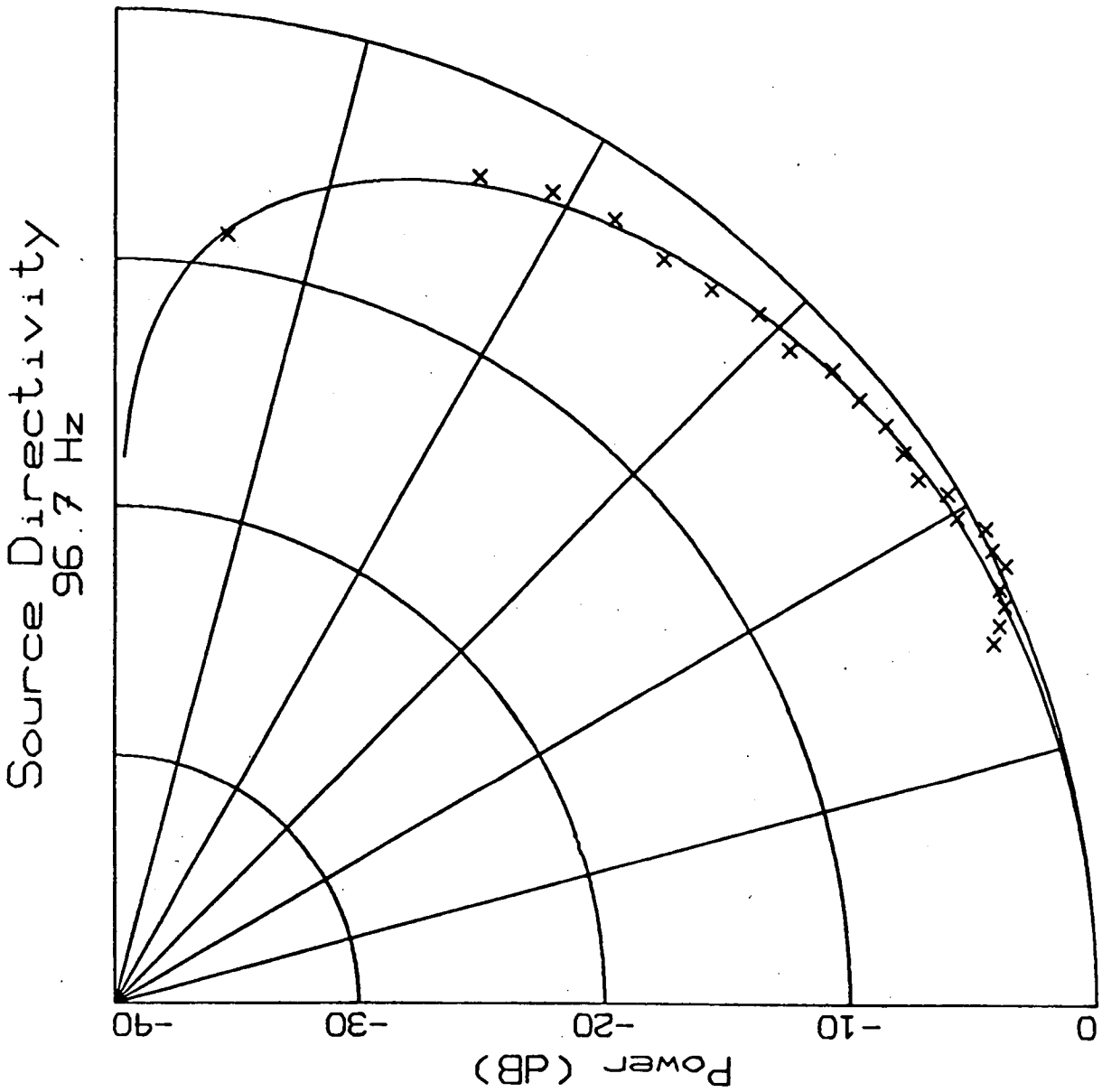

Figure 11a Directivity for Event at 500m Range
Showing Large Deviation from Multipole
Directivity Index $m = 0.58$ Shown for Comparison

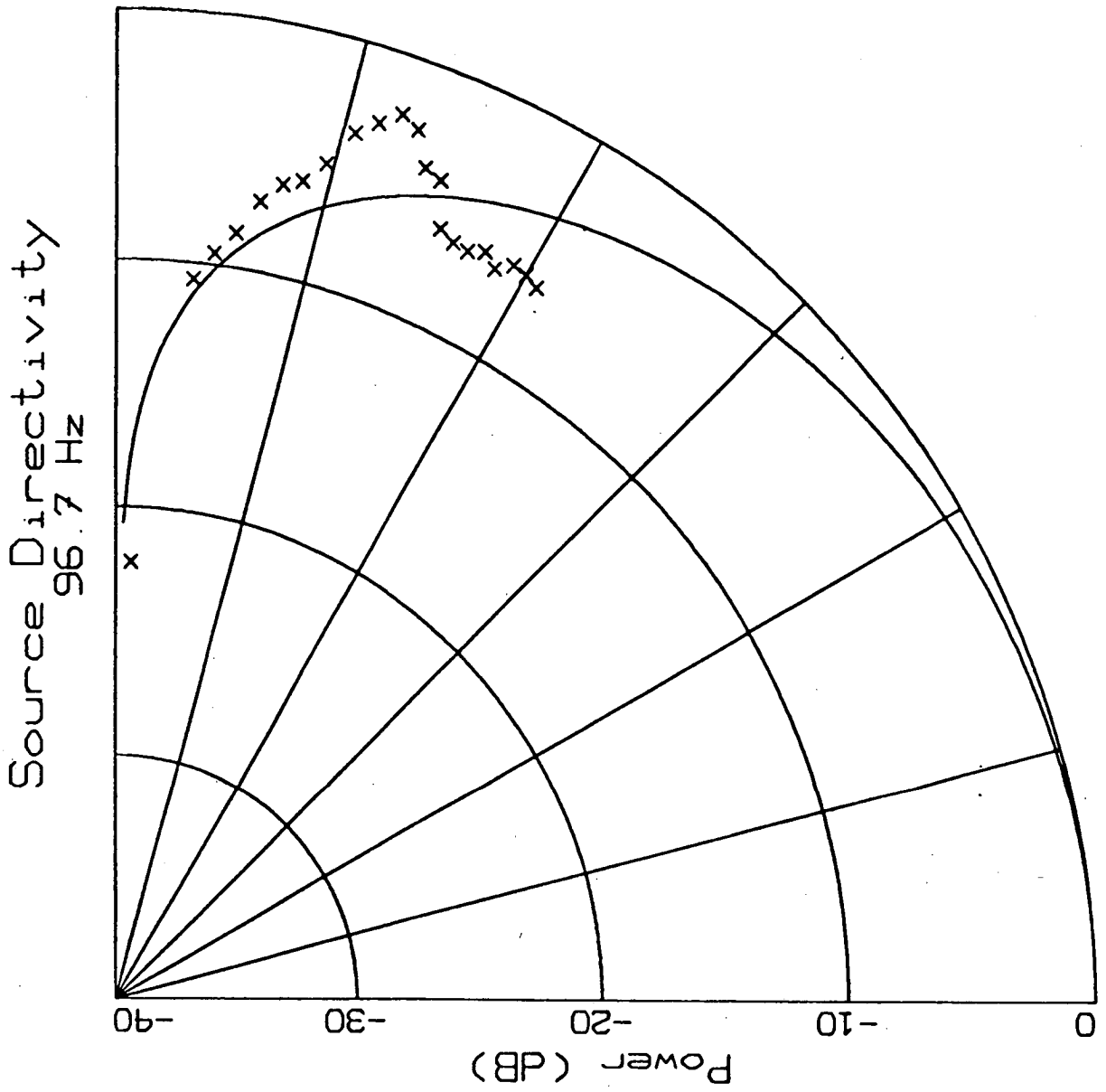

Figure 11b Directivity for Event at 250m Range
Showing Large Deviation from Multipole
Directivity Index $m = 0.29$ Shown for Comparison

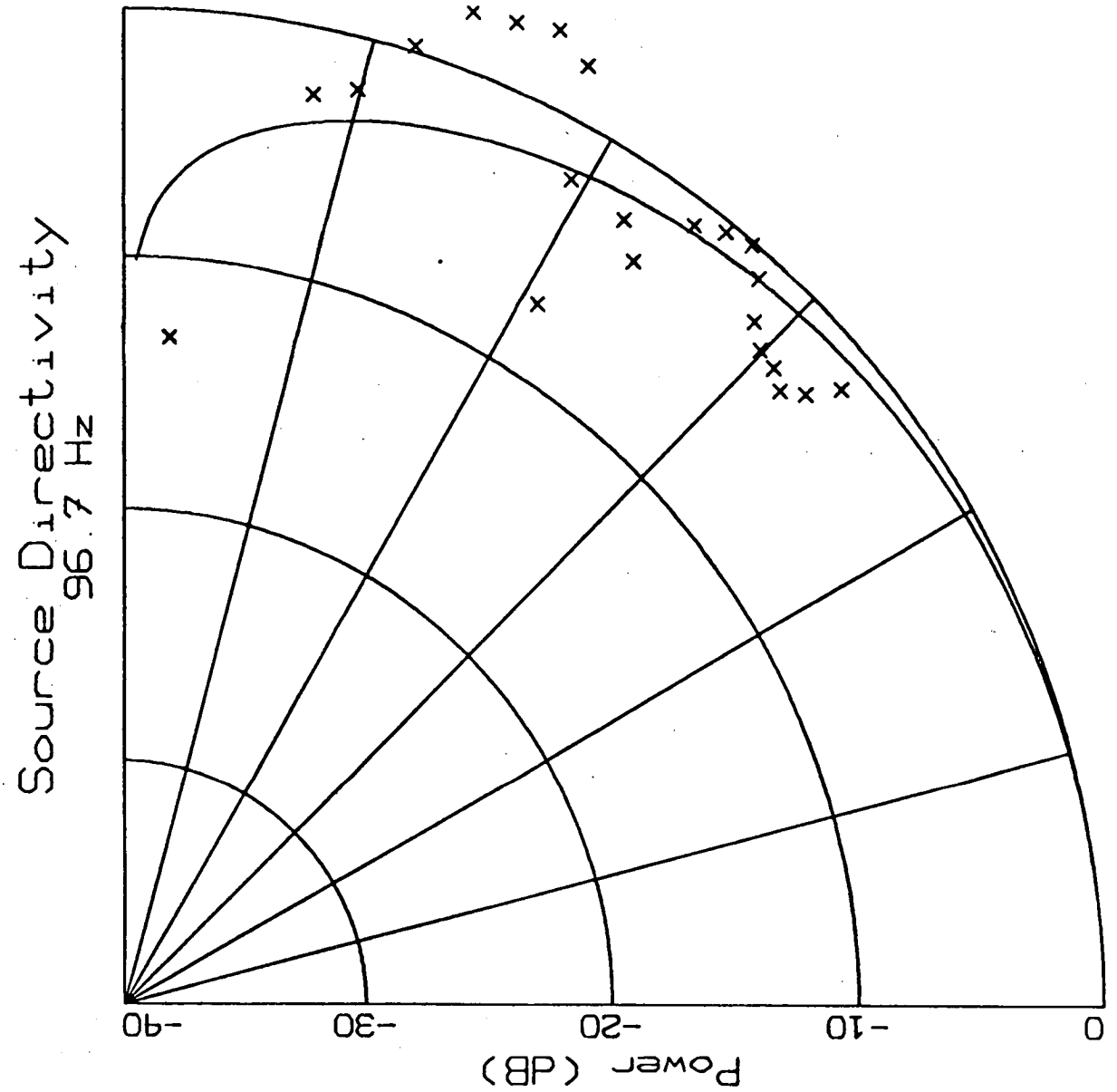

Figure 12 Distribution of Directivity Index m for All Events with 0m - 2000m Range

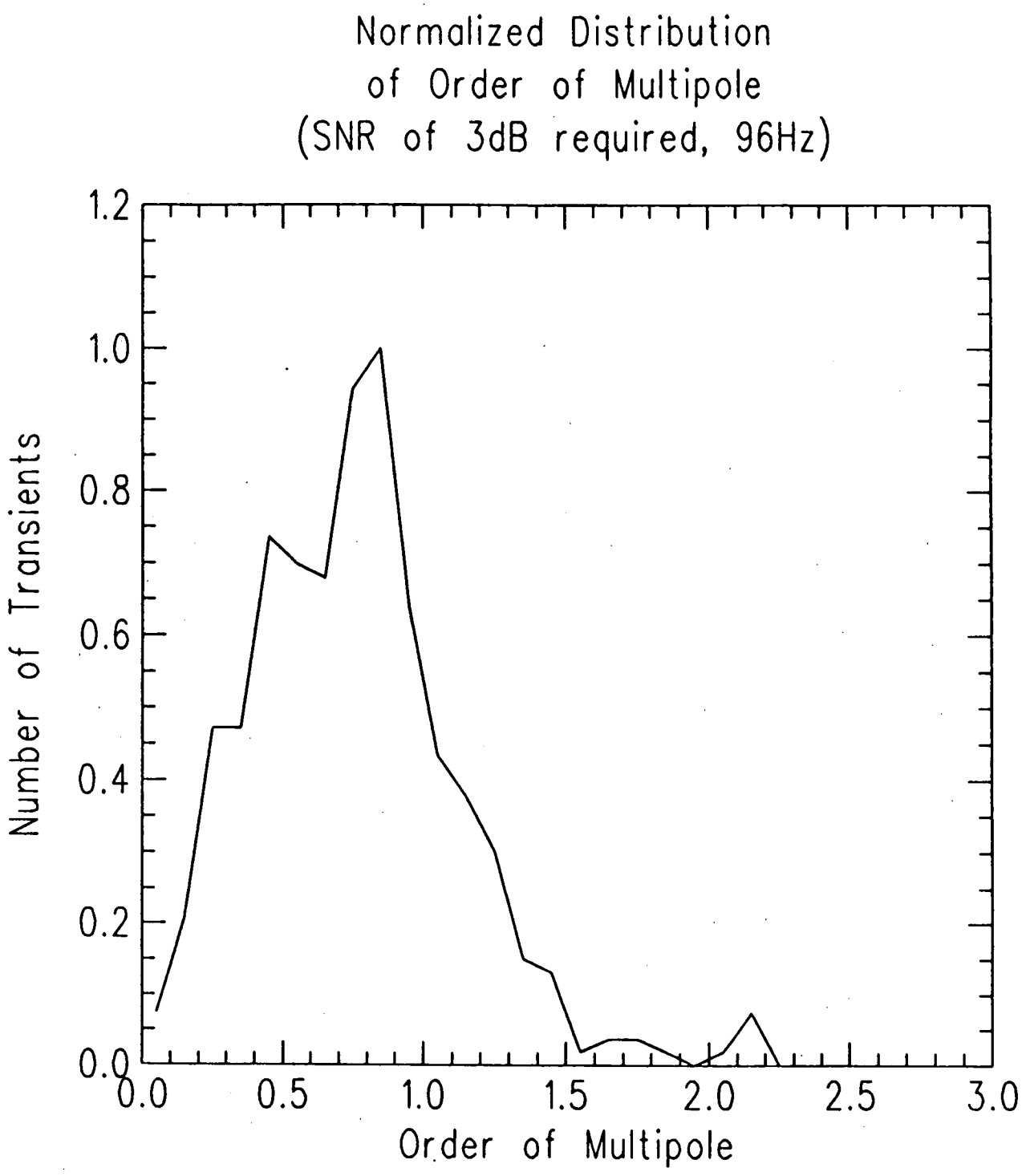

Figure 13

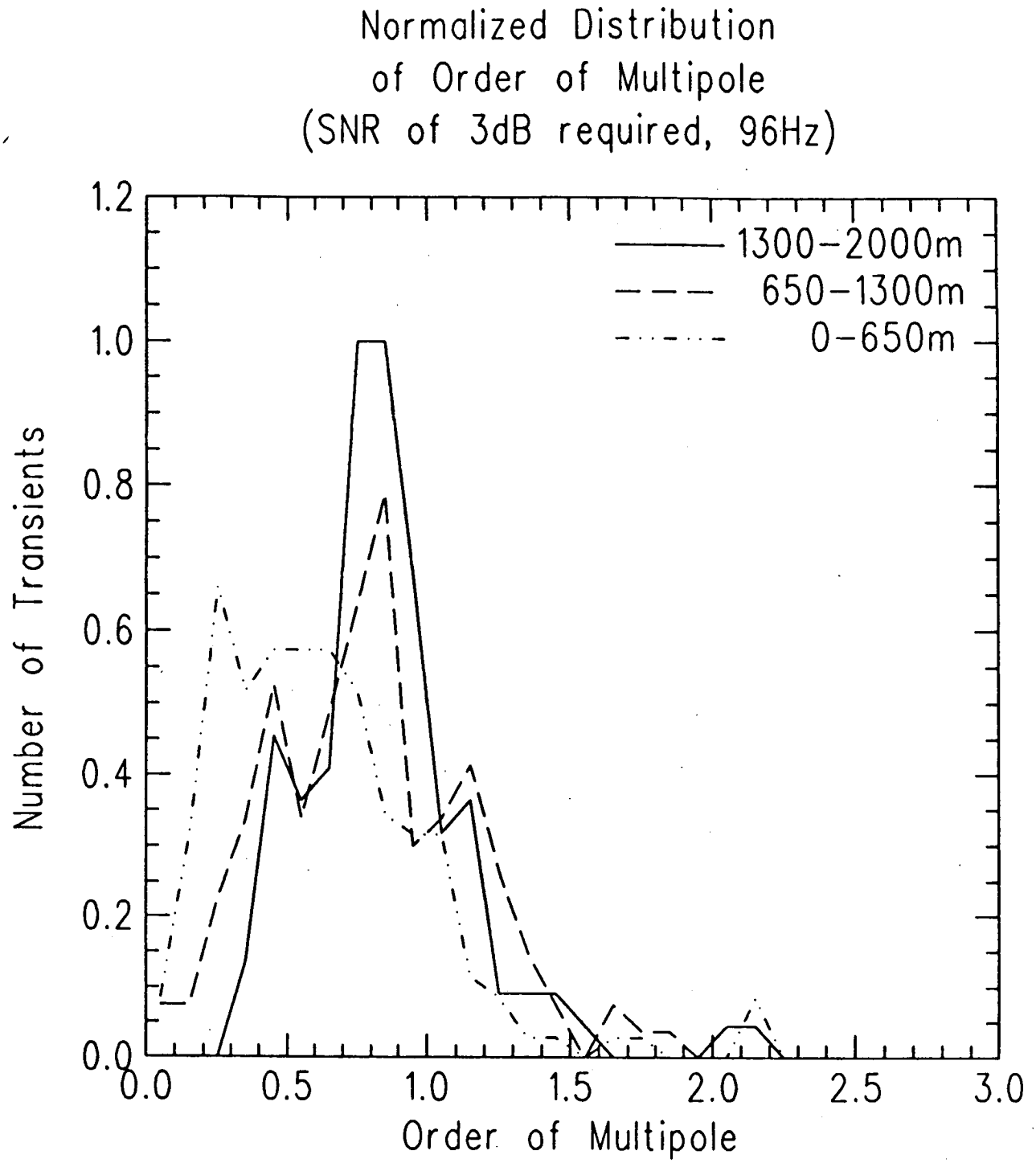
Normalized Distribution
of Order of Multipole
(SNR of 3dB required, 96Hz)
1300-2000m
650-1300m
0-650m
Number of Transients
Order of Multipole
0.0
0.2
0.4
0.6
0.8
1.0
1.2
0.0
0.5
1.0
1.5
2.0
2.5
3.0

Figure 14

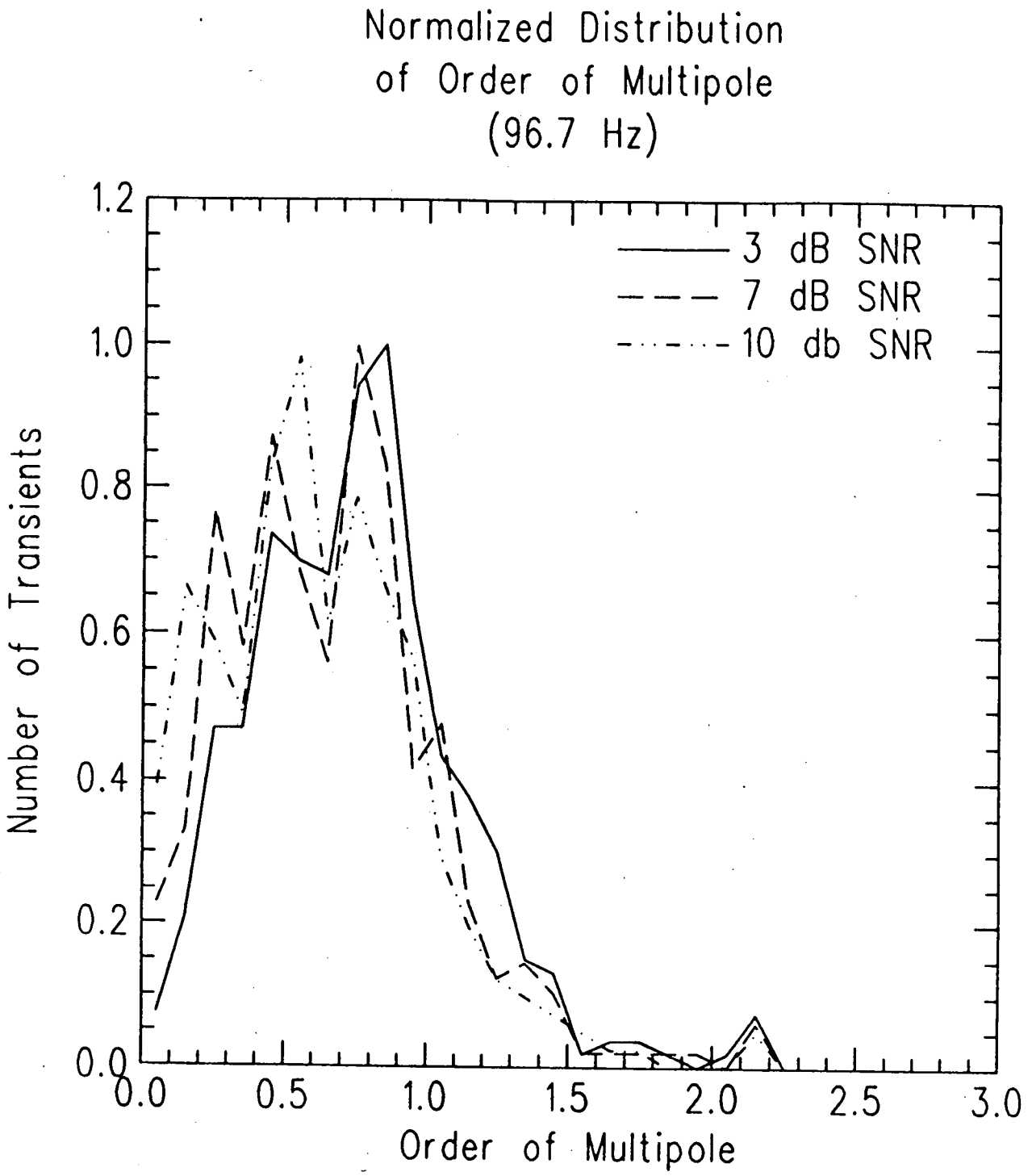
Normalized Distribution
of Order of Multipole
(96.7 Hz)
3 dB SNR
7 dB SNR
10 db SNR
Number of Transients
Order of Multipole
0.0
0.2
0.4
0.6
0.8
1.0
1.2
0.0
0.5
1.0
1.5
2.0
2.5
3.0

Figure 15

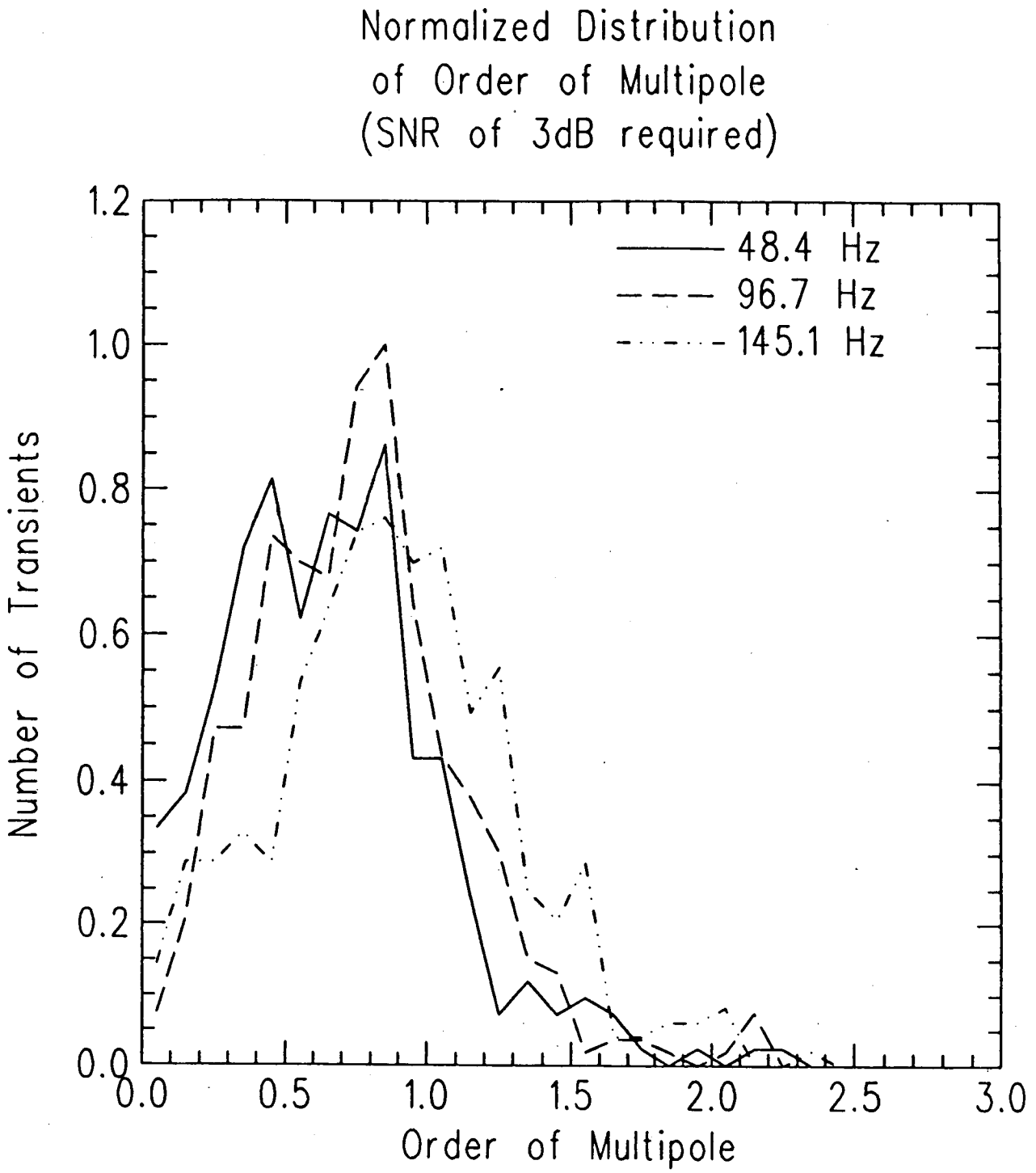
Normalized Distribution
of Order of Multipole
(SNR of 3dB required)
48.4 Hz
96.7 Hz
145.1 Hz
Number of Transients
Order of Multipole
0.0
0.2
0.4
0.6
0.8
1.0
1.2
0.0
0.5
1.0
1.5
2.0
2.5
3.0

INTRODUCTION

Detailed knowledge of the seabed properties are often needed in order to predict propagation characteristics in the ocean. The most useful parameters are the compressional and shear sound speeds. These two parameters are sufficient to totally characterize the reflection as a function of angle if the bottom is flat and no layering is present. However, layering or roughness of the bottom may modify the reflection function in a frequency-dependent manner. The techniques traditionally used to extract the seabed properties are: laboratory measurement of physical parameters of coring or grab samples, and *in-situ* acoustic reflection or refraction experiments. Analysis of samples provide unambiguous and precise values of physical properties of the substrata. Reflection and refraction measurements provide information about the acoustic effects of layering and roughness. Sources for reflection experiments are explosive charges, although Buckingham[1] has developed a technique in which the inter-sensor coherence of the ambient noise in shallow water is used to determine the critical angle of the seabed. Unfortunately, the environmental model Buckingham used does not include shear, and the difference in loss between the regions below and above critical angle must be large for the technique to be used successfully.

The concept of making use of the ambient noise as an acoustic source is appealing, as it eliminates the time-consuming task of deploying charges. This is a problem especially in the Arctic environment, where one must cut through the thick (3 - 7 meters) Arctic pack ice in order to drop the charges. The harsh weather conditions in the Arctic often makes it difficult to operate drilling equipment. Thus, this technique which requires only one hole in the ice for deployment of the vertical array, may help increase the possible number of sites surveyed.

In this paper, a technique is described for measuring the reflection coefficient of the Arctic seabed as a function of angle with a single vertical array of hydrophones. Naturally occurring ice cracks were used as acoustic sources. A complication arises compared to the use of charges as sources, since the ice cracks have a source directivity. This directivity can usually be described as a multipole; however, the order of the multipole may vary from crack to crack. Thus one must

first extract the source directivity index from the direct path before extrapolating to the higher angles of the bottom paths. The range of the source is first determined by comparing the difference in arrival times across the array with those predicted by a ray-based model using both the direct arrival and the multiple reflections from the seabed and underice surface. Then the source directivity index is determined using the direct arrival path only, assuming that the source directivity follows the form of a multipole. The expected power at angles corresponding to the bottom path is extrapolated using the source directivity index thus calculated. A plot of the reflection coefficient versus grazing angle clearly indicates the value of the critical angle.

I. ENVIRONMENT AND INSTRUMENTATION

The measurements were made in April 1988 with a 22-element vertical array suspended from the Arctic pack ice, off the North coast of Ellesmere Island, Canada, in 420 meters of water. The sound speed of the bottom was independently estimated through a bottom grab sample[2] and an acoustic seismic refraction survey[3]. The bottom grab sample consisted of sand (quartz). The bottom sound speeds inferred from these measurements are displayed in Table I. The sound speed profile at the site is shown if Fig. 1. The recordings of ambient noise used for the present study were made over a period of six days, during which the temperature fluctuated from a minimum of -40°C to a maximum of -14°C. The ice cracking events were extracted from a set of approximately 60 two-minute samples of ambient noise taken during this six day period.

The hydrophones used for this project were the 22 hydrophones on the vertical portion of the array. These hydrophones were spaced 12 meters apart, with the top hydrophone 18 m below sea level. The acoustic pressure was sampled at the rate of 516 Hz, with a low-pass filter at 150 Hz.

TABLE I. Density and compressional sound speed measured at the site of recording, from a bottom grab sample and a seismic refraction survey, using the head wave around 200 Hz.

Method	depth	density	sound speed
Grab sample	6 cm	2.14 gr/cm^3	1794 m/s
Grab sample	14 cm	2.13 gr/cm^3	1683 m/s
Seismic refraction	~10 m		1980 ± 18 m/s

II. METHOD

The two methods used automatically to detect transients in the time series are described in separate publications[4,5]. Once the transients are detected, they are inspected visually in a multi-channel time-series display (see Fig. 2) in order to eliminate false alarms, and extract intervals containing the direct and bottom-bounce arrivals. The range of each source is found by comparing the time delays of the arrivals with those predicted by a ray propagation model. The time series intervals for both the direct and bottom-bounce paths are Fourier-transformed, and the power in octave-wide bands averaged together. The data reported below are for the octave band centered on 96 Hz. The power in each channel is corrected for geometrical spreading and the ambient noise. The noise is removed by subtracting the power from an equal length of data immediately preceding the direct arrival. For our measurements, the noise power was only sampled at one hydrophone and assumed constant along the array. The power contribution from the direct path is modeled as a multipole, i.e. with a power angular dependence of the following form:

$$P_r = P_s \sin^m(\theta). \tag{1}$$

Over 80% of the 160 transients identified fit the multipole model closely. The parameters m and P_s are found for each event using least-mean-squared fitting applied to the logarithm of the power of the direct arrival at each hydrophone. Those events which are found to fit the multipole model well are used to extract the reflectivity function from the seabed. This is done by comparing the power

measured in the bottom-bounce arrivals at each hydrophone with that predicted by extrapolating from (1) using the parameters m and P_s extracted from the direct arrivals (Fig. 3). The difference between the measured power and the predicted power extrapolated from the directarrivals is assumed to be the loss due to reflectivity at the seabed. The arrival at each hydrophone corresponds to a different bottom scattering angle which is calculated using the ray propagation model mentioned above. Thus, the reflectivity can be plotted against the bottom grazing angle as shown in Fig. 4.

III. RESULTS

The bottom reflectivity function measured for each event at each hydrophone, according to the method described in the last section, is shown in Fig. 4 as a scatter diagram. Despite the large spreading in reflectivity, one can easily discern that the critical angle, defined as the angle at which the reflectivity begins to drop, occurs somewhere between 35° and 40° grazing angle. In order to make the extracted directivity function more explicit, the measured values are averaged using a window 3° wide. The reflectivity function thus averaged is displayed in Fig. 5. The averaged reflectivity value below the critical angle is just below 1.0, and very stable. The critical angle is now seen to occur around 35°. The relation between the critical grazing angle θ_c and the ratio of the water compressional velocity c_w and that of the seabed c_s is

$$\cos(\theta_c) = c_w / c_s . \tag{2}$$

Since $c_w = 1457$ m/s, the compressional velocity of the seabed inferred from this critical angle measurement is $c_s = 1779$ m/s. This can be compared with the velocity measurements made from the bottom grab sample and the refraction measurements in Table I.

A rise in the reflectivity function around 60° is also very noticeable. This rise is not actually due to an increased reflectivity function at this angle, but is an artifact due to the use of an incomplete source directivity function (Eq. 1) which does not include the leaky plate wave radiating

around 60° from the ice at the site. If the source emits more power at high angles than the model source function of Eq. 1 predicts, the difference between the measured and predicted power will be greater than it should, and will show up in the reflectivity function. The extra source power due to the plate wave may now be quantified. It corresponds to a power of 3 dB above the pure multipole source (from a reflectivity of 0.2 to 0.4), with an approximately Gaussian distribution centered on 60° and a standard deviation of 5°. The radiation angle θ_p of a leaky plate wave into the water below corresponds to the critical angle between the two media. A grazing angle of 60° at the water-seabed interface corresponds to a source angle of 60.5°. The leaky ice plate wave speed is thus found to be 2914 m/s.

IV. DISCUSSION

A. Sources of error

Several factors contribute to errors in both the grazing angle and the reflectivity value. Since the duration of each arrival is of finite length, it happens in some cases that the direct and bottom-bounce partially overlap. A boundary is nonetheless placed between the two arrivals, and therefore some of the direct arrival's power will be assigned to the bottom-bounce arrival. The power for the direct arrival is underestimated, and that for the bottom-bounce overestimated. This tends to happen for only a few channels toward the bottom of the array for distant events, since this is where the interarrival delay is at a minimum.

The main source of scatter in Fig. 4 is due to misfit of the value of the multipole order m. A slight misfit in the value of m at the low angles corresponding to direct arrivals leads to a rather large difference in the extrapolated power at the larger angles corresponding to bottom-bounce angles. However, this error in extrapolation of the expected bottom-bounce power leads to a systematic error in the reflectivity function for one given event. To make this evident, the reflectivity function for a few events for the arrival at each hydrophone is plotted in Fig. 6, where the arrivals corresponding to one single event are joined together by a broken line. One may now notice that although there can be a large difference in the reflectivity value corresponding to

different events arriving at the same angle, the scatter around the mean for a single event is much smaller.

This residual scatter within a single event is thought to correspond to the irreducible error in measurement due to the relatively poor signal-to-noise ratio, of between 3 and 10 dB. Moreover, since the same estimate of noise level is used for each channel, small fluctuations of the ambient noise level with depth, or inequalities in absolute calibration at each channel, would lead to further random inequalities between channels.

The estimate of angles depends entirely on estimating time delays between different channels for a given arrival. If this can be done to an accuracy of one sampling point, for a given channel, then the accumulated error across the array leads to a error on angle measurements of the order of 2.3° corresponding to an error in c_s of 45 m/s.

B. Comparison with other measurements

The value of the compressional sound speed in the seabed obtained from the critical angle can be compared with those obtained by two other methods in Table I. The value extracted in the present study compares rather well with those obtained from the bottom grab sample. However, it does not agree very well with that obtained from the seismic refraction survey. The nature of this discrepancy is unknown.

The value for the leaky plate wave speed can be compared to a direct measurement made at the site by Ozard and Brooke[6] using a hammer and geophones. The speed they obtained is 3050 ± 100 m/s. The error interval for the value obtained from the present study overlaps with that obtained by Ozard and Brooke.

C. Leaky plate wave

The study of source directivity through direct arrivals power measurement[4] yielded very little data on the relative strength and width of the leaky plate wave contribution. This is because very few events occur close enough to the array for the direct arrival to occur at 60° or more.

Better statistics are available through the present study, since it corresponds to a much larger number of arrivals, because bottom-bounce events with a source angle of around 60° arriving at the array lay on a much larger circle around the array, and comprises more surface. In this study, this power shows up as an artifact in the reflectivity function, which would not happen if this extra power was included in the source model instead. This would be desirable, since one wants the reflectivity function derived through this method to represent the true reflectivity function of the seabed. A new source directivity model as tentatively proposed from the results of the last section is the sum of the multipole contribution and the leaky plate wave contribution represented by a Normal function,

$$P_r = P\left[\sin^m\theta + C\exp\left(-\frac{(\theta-\theta_L)^2}{2w^2}\right)\right]. \tag{3}$$

where C is a constant giving the relative contributions of the acoustic mode and the leaked longitudinal plate wave, and θ_L and w are the critical angle and beamwidth of the leaked longitudinal plate wave respectively. For our data, $C \approx 1.0$, $\theta_L \approx 60°$, and $w \approx 5°$. However, it is not known whether the relative power and radiating angle of the plate wave will be the same in other ice cover conditions. On the encouraging side, Brooke[7] reported that the leaky plate wave speed was almost the same (~2950 m/s) in 2.5m thick new ice, as it was at the present ice in much thicker ice.

V. CONCLUSIONS

It has been shown in this paper that it is possible to use local ice cracking with a vertical array of hydrophones to measure the reflectivity of the seabed as a function of reflection angle. The critical angle at the seabed interface is easily extracted from the reflectivity function, and yields the sediment sound speed. The steps involved in using this method are: detect and isolate ice cracking events, determine the range of each event using a ray tracing model, separate the direct

arrival and the bottom-bounce arrival from each other and higher order arrivals, subtract the noise contained in an interval of time before the events, fit the direct arrival power at each hydrophone to the source directivity model in order to extract the parameter m, extrapolate the power to that expected at angles corresponding to bottom-bounce paths, and the difference between the expected and the measured bottom-bounce power is assumed to be due to reflection loss at the seabed. The method is fairly time-consuming however, and it may take several days for a trained operator to extract the full directivity function at one site. The amount of recording needed depends entirely on the frequency of ice cracking at the time of recording. During some periods, no ice cracking is taking place at all, and the ambient noise is totally stationary. At some other times, one event occurs every few seconds, and a few minutes of data may be all what is needed to make the reflectivity measurements.

In order to accommodate the leaky plate wave which was introducing an artifact in the reflectivity function due to the use of an incomplete model of the source directivity, a more complete source directivity function is proposed. It contains both the multipole source and a contribution from the leaky plate wave peaking at 60°, with a normal distribution having a standard deviation of 5°.

REFERENCES

1. Buckingham, M.J., and Jones, S.A.S. "A New Shallow-Ocean Technique for Determining the Critical Angle of the Seabed from the Vertical Directionality of the Ambient Noise in the Water Column," J. Acoust. Soc. Am. **81**, 938-946 (1987).

2. L. A. Mayer and J. Marsters, "Measurement of geophysical properties of Arctic sediment cores," DREP Contractors Report 89-19 (1989).

3. J. P Todoeschuck, J. M. Ozard, and J. M. Thorleifson, "Refraction and reflection experiments with a vertical array of hydrophones in the Lincoln Sea," (A), Eos, **69**, 1320 (1988).

4. M.V. Greening, P. Zakarauskas, and R.I. Verrall, "Vertical directivity measurements of ice cracking," Submitted to J. Acoust. Soc. Am. (1990).

5. P. Zakarauskas, C. J. Parfitt, and J. M. Thorleifson, "Statistics of transients in Arctic ambient noise," To be published in the proceedings of the First French Conference on Acoustics, Lyon, France (1990).

6. G.H. Brooke and J. M. Ozard, Personnal Communication.

7. G.H. Brooke and J. M. Ozard, "In-situ measurement of elastic properties of sea ice," in Underwater Acoustic Data Processing, edited by Y.T. Chan (Kluwer Academic Pub., Dordrecht, The Netherlands, 1989), pp. 113-118.

LIST OF FIGURES

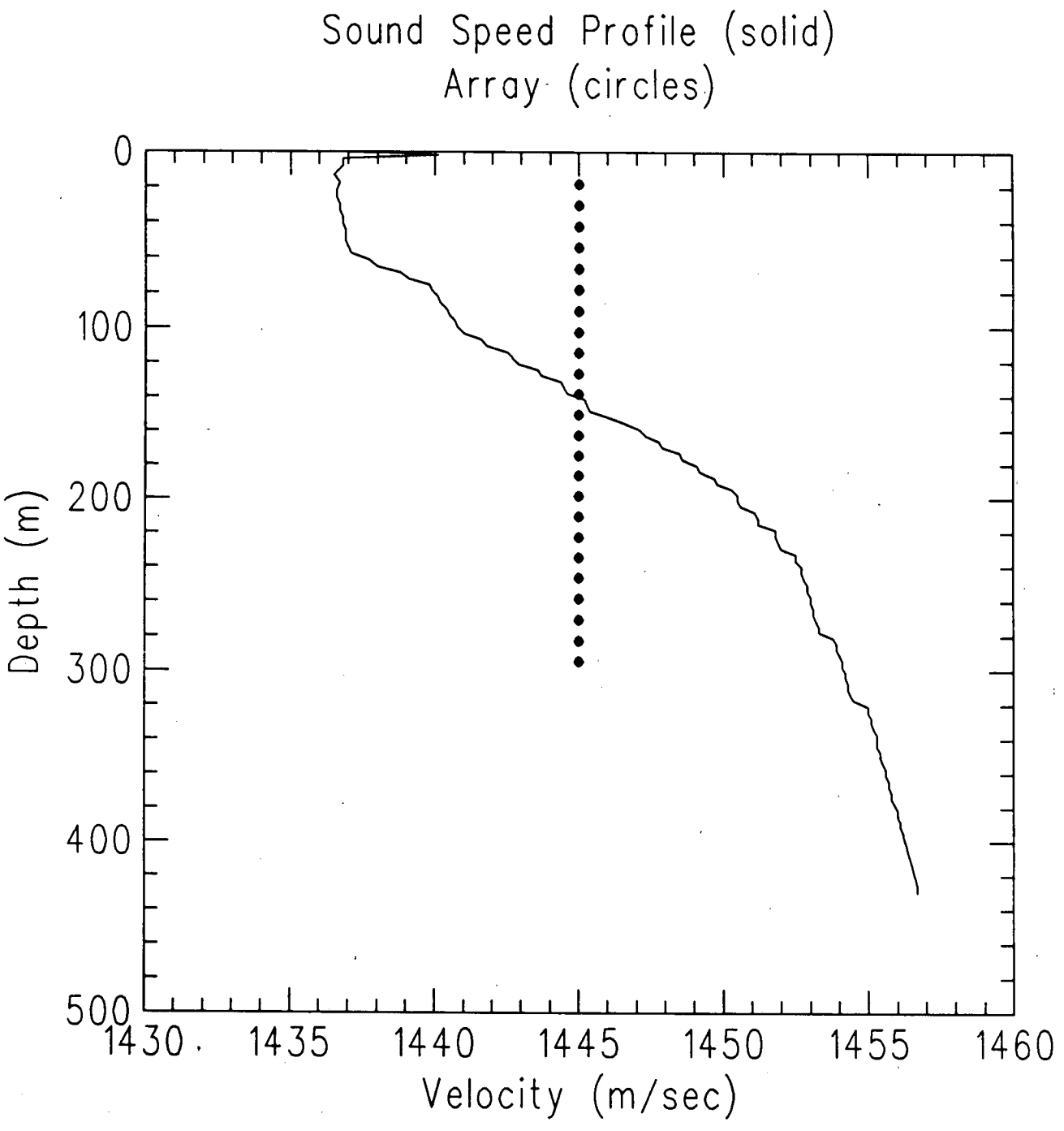
Sound Speed Profile (solid)
Array (circles)
0
100
200
300
400
500
Depth (m)
1430
1435
1440
1445
1450
1455
1460
Velocity (m/sec)

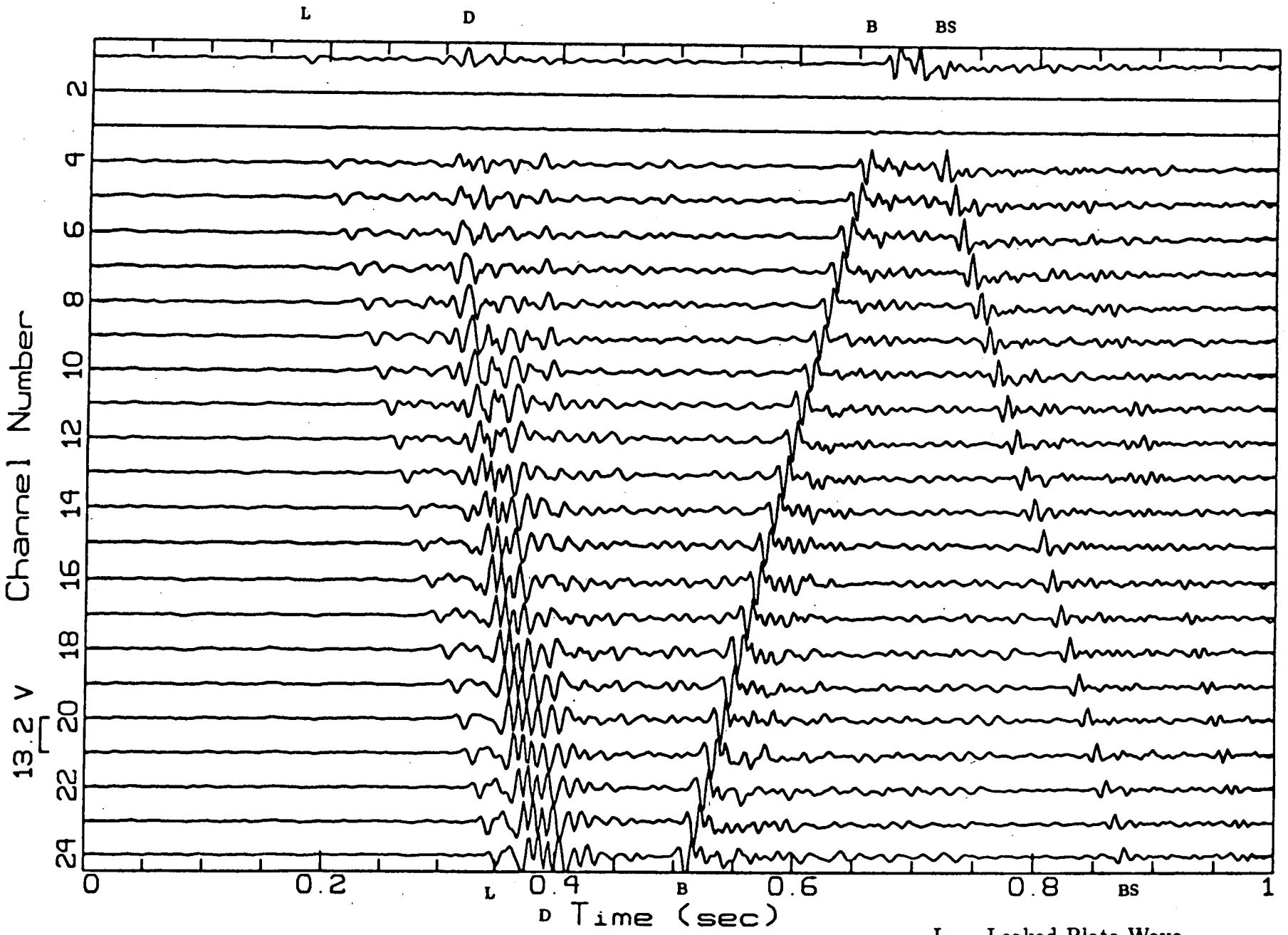

Ice Cracking Event with
Leaked Longitudinal Plate Wave
Source Range = 400 m

L - Leaked Plate Wave
D - Direct Arrival
B - Bottom Reflection
BS - Bottom Surface Reflection

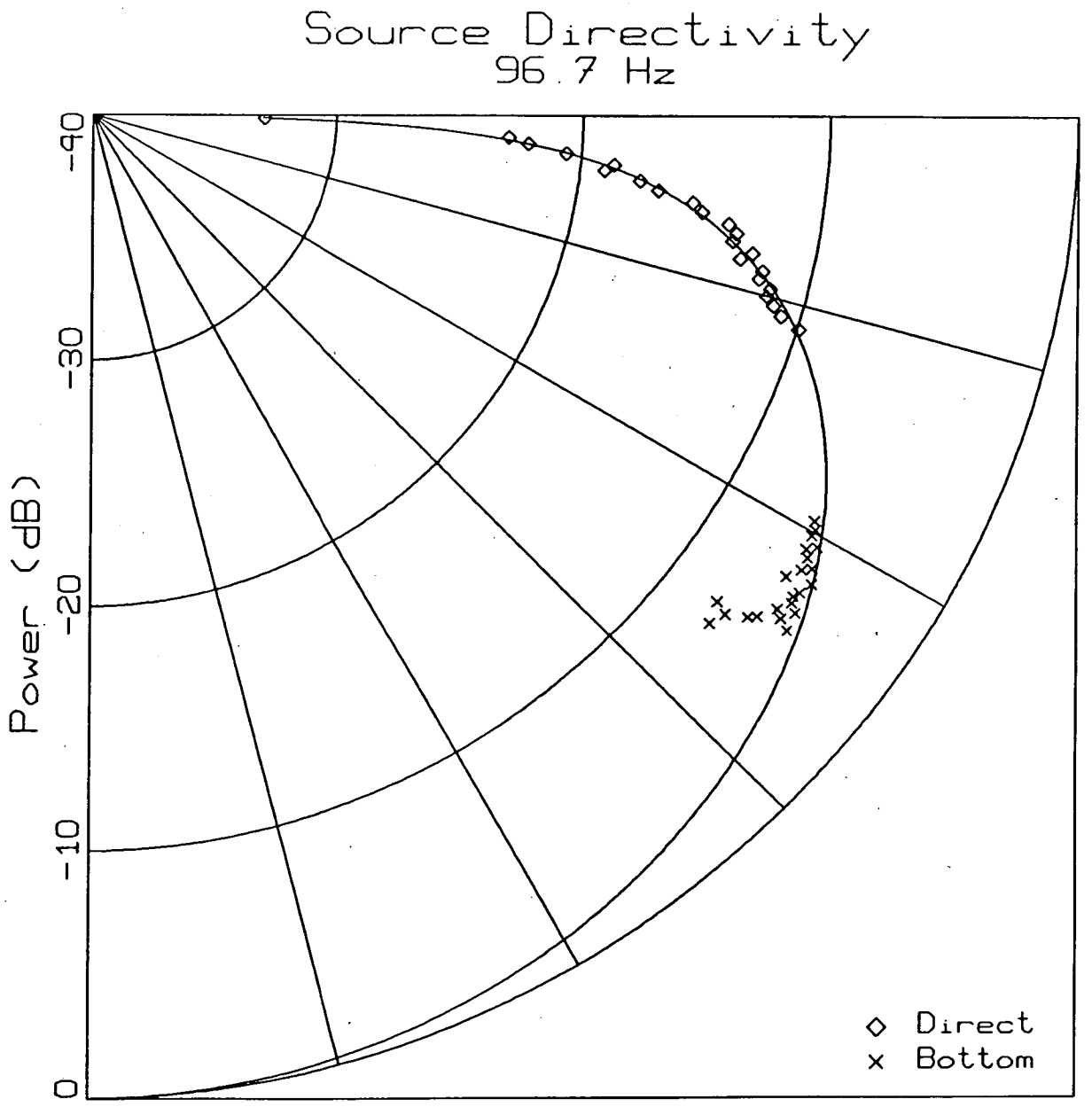
Source Directivity
96.7 Hz
Power (dB)
-90
-30
-20
-10
0
Direct
Bottom

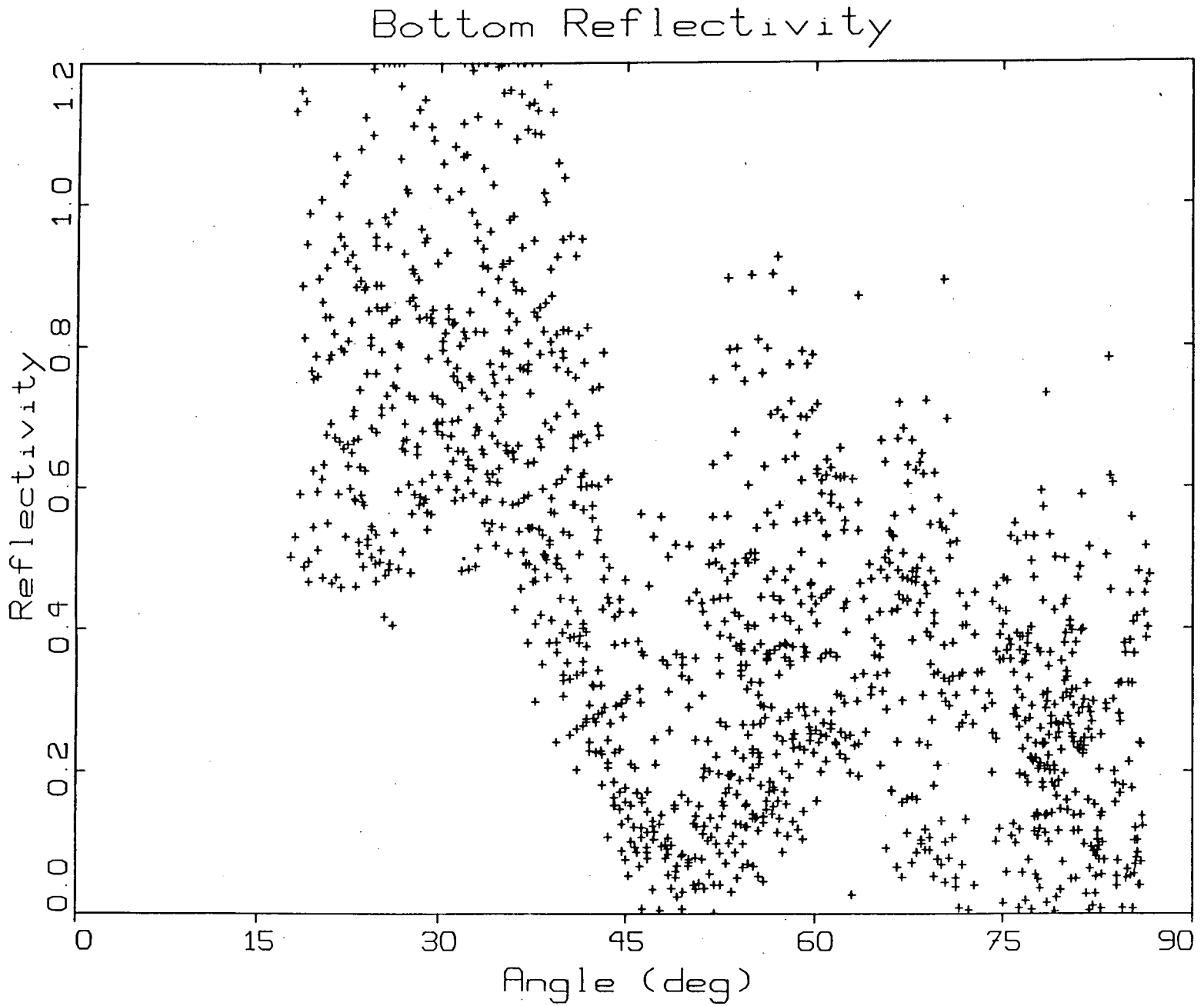
Bottom Reflectivity
Reflectivity
0.0
0.2
0.4
0.6
0.8
1.0
1.2
0
15
30
45
60
75
90
Angle (deg)

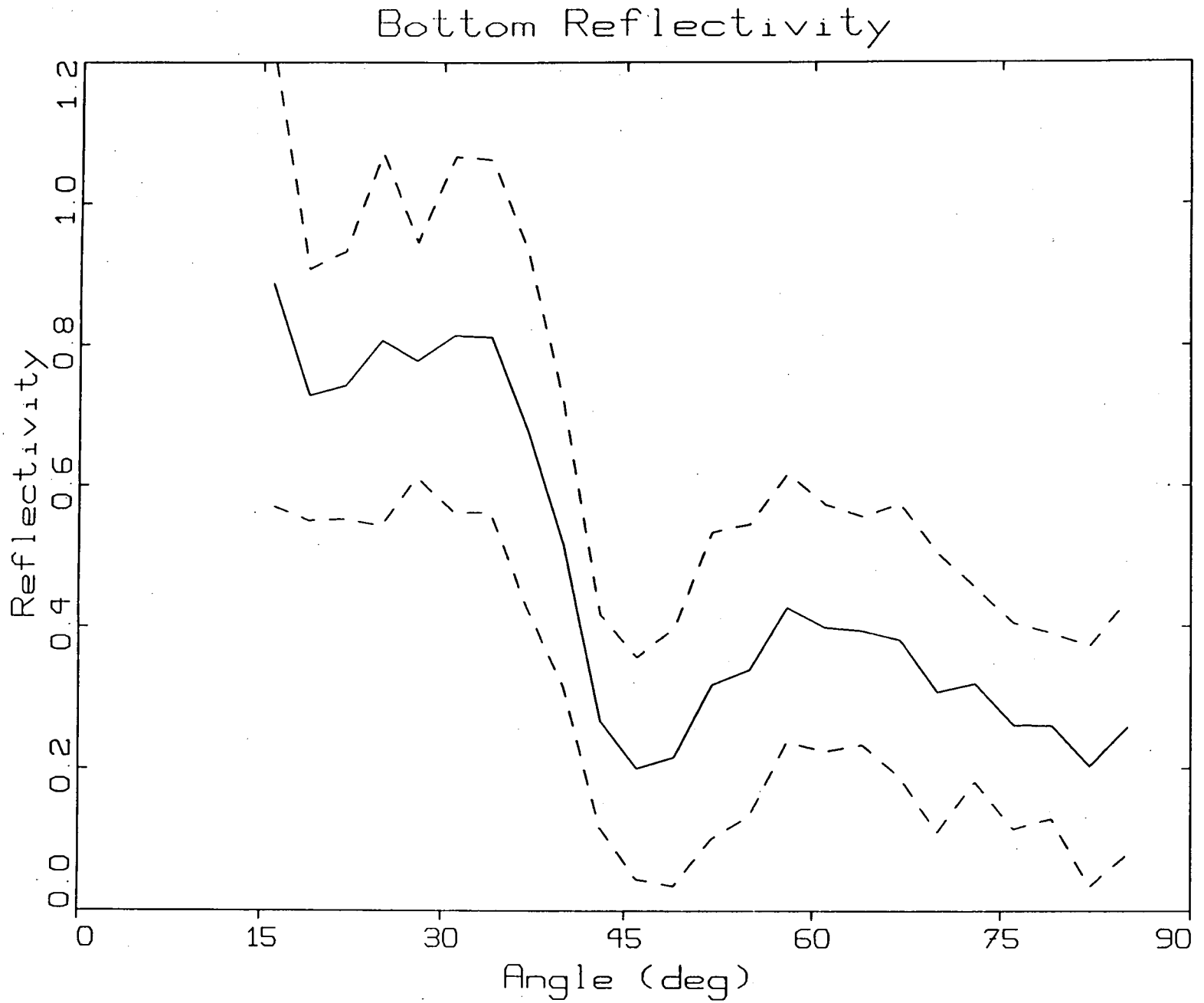
Bottom Reflectivity
Reflectivity
0.0
0.2
0.4
0.6
0.8
1.0
1.2
0
15
30
45
60
75
90
Angle (deg)

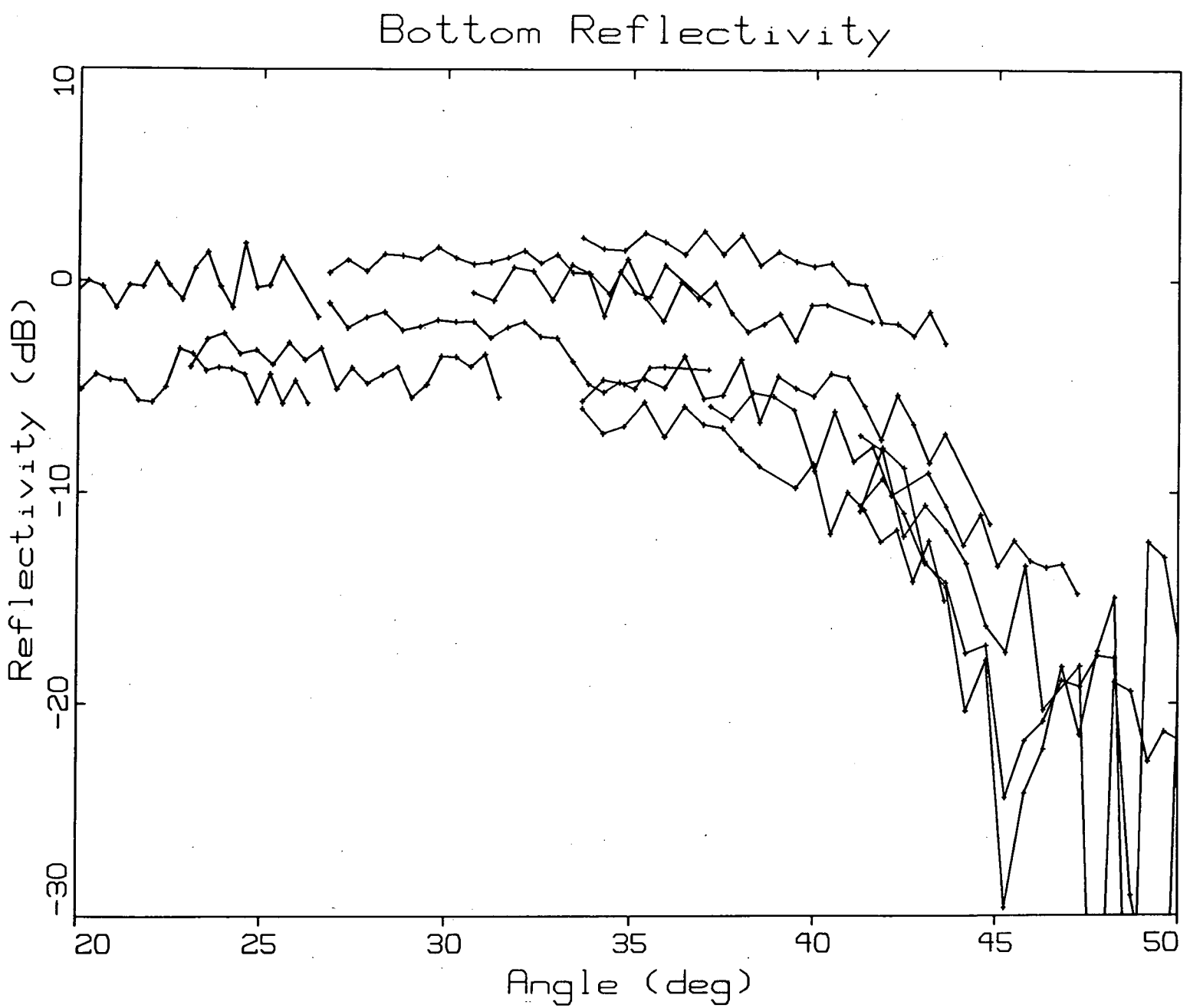
Bottom Reflectivity
Reflectivity (dB)
10
0
-10
-20
-30
20
25
30
35
40
45
50
Angle (deg)

DOCUMENT CONTROL DATA

(Security classification of title, body of abstract and indexing annotation must be entered when the overall document is classified)

1. ORIGINATOR (the name and address of the organization preparing the document. Organizations for whom the document was prepared, e.g. Establishment sponsoring a contractor's report, or tasking agency, are entered in section 8.)

Jasco Research Ltd.,
#102 - 9865 W. Saanich Road
Sidney B. C. V8L 3S1

2. SECURITY CLASSIFICATION (overall security classification of the document. including special warning terms if applicable)

Unclassified

3. TITLE (the complete document title as indicated on the title page. Its classification should be indicated by the appropriate abbreviation (S,C or U) in parentheses after the title.)

Arctic Ambient Noise and Modeling.

4. AUTHORS (Last name, first name, middle initial)

Greening,V. Michael

5. DATE OF PUBLICATION (month and year of publication of document)

March 30 1990

6a. NO. OF PAGES (total containing information. Include Annexes, Appendices, etc.)

56

6b. NO. OF REFS (total cited in document)

31

7. DESCRIPTIVE NOTES (the category of the document, e.g. technical report, technical note or memorandum. If appropriate, enter the type of report, e.g. interim, progress, summary, annual or final. Give the inclusive dates when a specific reporting period is covered.)

Contractor Report No. 90-16

8. SPONSORING ACTIVITY (the name of the department project office or laboratory sponsoring the research and development. Include the address.)

DREP, Forces Mail Office, Victoria B. C. V0S 1B0

9a. PROJECT OR GRANT NO. (if appropriate, the applicable research and development project or grant number under which the document was written. Please specify whether project or grant)

9b. CONTRACT NO. (if appropriate, the applicable number under which the document was written)

W7708-8-0904/01-XSB

10a. ORIGINATOR'S DOCUMENT NUMBER (the official document number by which the document is identified by the originating activity. This number must be unique to this document.)

10b. OTHER DOCUMENT NOS. (Any other numbers which may be assigned this document either by the originator or by the sponsor)

11. DOCUMENT AVAILABILITY (any limitations on further dissemination of the document, other than those imposed by security classification)

(X) Unlimited distribution
( ) Distribution limited to defence departments and defence contractors; further distribution only as approved
( ) Distribution limited to defence departments and Canadian defence contractors; further distribution only as approved
( ) Distribution limited to government departments and agencies; further distribution only as approved
( ) Distribution limited to defence departments; further distribution only as approved
( ) Other (please specify):

12. DOCUMENT ANNOUNCEMENT (any limitation to the bibliographic announcement of this document. This will normally correspond to the Document Availabilty (11). However, where further distribution (beyond the audience specified in 11) is possible, a wider announcement audience may be selected.)

Unclassified

13. ABSTRACT (a brief and factual summary of the document. It may also appear elsewhere in the body of the document itself. It is highly desirable that the abstract of classified documents be unclassified. Each paragraph of the abstract shall begin with an indication of the security classification of the information in the paragraph (unless the document itself is unclassified) represented as (S), (C), or (U). It is not necessary to include here abstracts in both offical languages unless the text is bilingual).

This report is composed of two papers for submission to a journal, plus some preliminary results. The first paper, "Vertical directivity measurements of ice cracking", reprots the results of fitting the directivity of 160 events with a multipole function. The events were collected in the Arctic ocean during sprintime with a vertical array of 22 elements. The second paper, "Extraction of the seabed reflectivity function using ice cracking noise as a signal source", applies the results of the first paper to bottom-reflected energy. The adendum is entitled "Source distribution" reports the spatial localization of the sources.

14. KEYWORDS, DESCRIPTORS or IDENTIFIERS (technically meaningful terms or short phrases that characterize a document and could be helpful in cataloguing the document. They should be selected so that no security classification is required. Identifiers, such as equipment model designation, trade name, military project code name, geographic location may also be included. If possible keywords should be selected from a published thesaurus. e.g. Thesaurus of Engineering and Scientific Terms (TEST) and that thesaurus-identified. If it is not possible to select indexing terms which are Unclassified, the classification of each should be indicated as with the title.)

AMBIENT NOISE
ICE CRACKING
SOURCE DIRECTIVITY
REFLECTIVITY FUNCTION
ARCTIC ACOUSTICS